A Serum- and Feeder-Free System to Generate CD4 and Regulatory T Cells from Human iPSCs

Authors

Helen Fong[1], Matthew Mendel[1], John Jascur[1], Laeya Najmi[1], Ken Kim[1], Garrett Lew[1], Swetha Garimalla[1], Suruchi Schock[1], Jing Hu[1], Andres Villegas[1], Anthony Conway[1,2], Jason Fontenot[1], Simona Zompi[1]

Affiliation

[1] Sangamo Therapeutics, 7000 Marina Blvd, Brisbane, CA 94005; 501 Canal Blvd. Richmond, CA 94804

[2] Current affiliation: Replay, 5555 Oberlin Drive, Unit 120, San Diego, CA 92121

Corresponding authors

Helen Fong: hfong82@gmail.com

Simona Zompì: simona.zompi@gmail.com

Abstract

iPSCs can serve as a renewable source of a consistent edited cell product, overcoming limitations of primary cells. While feeder-free generation of clinical grade iPSC-derived CD8 T cells has been achieved, differentiation of iPSC-derived CD4sp and regulatory T cells requires mouse stromal cells in an artificial thymic organoid. Here we report a serum- and feeder-free differentiation process suitable for large-scale production. Using an optimized concentration of PMA/Ionomycin, we generated iPSC-CD4sp T cells at high efficiency and converted them to Tregs using TGFβ and ATRA. Using zinc finger nucleases, we demonstrated high non-viral, targeted integration of an HLA-A2 CAR in iPSCs. iPSC-Tregs +/- HLA-A2 CAR phenotypically, transcriptionally and functionally resemble primary Tregs and suppress T cell proliferation *in vitro*. Our work is the first to demonstrate an iPSC-based platform amenable to manufacturing CD4 T cells to complement iPSC-CD8 oncology products and functional iPSC-Tregs to deliver Treg cell therapies at scale.

Introduction

Engineered autologous T cell therapies have shown the ability to transform the oncology field, yet producing these products at scale for large numbers of patients has proven difficult. The ability to derive hypoimmunogenic engineered T cells from self-renewing human induced pluripotent stem cells (iPSCs) could dramatically increase access to these therapies [1]. The advantages of using iPSCs over primary cells include the capacity to easily multiplex edit the starting cell source, access to a self-renewable and well-characterized product, and standardization of the product through the development of a master cell bank (MCB). However, while using iPSCs as source material can have numerous benefits in terms of standardization and scale-up, differentiation of T cells from iPSCs has been challenging.

Access to a self-renewable, potentially unlimited source of cells is particularly attractive for cell types that are difficult to isolate or present in small numbers, such as regulatory T cells (Tregs). In recent years there has been much interest in the use of Tregs to treat a wide variety of diseases, including autoimmune disorders, as well as in organ transplantation [2]. As of 2022, there were more than 30 active and completed clinical trials testing the safety and efficacy of Treg cell therapies [3]. Most of the studies have focused on *in vitro*-expanded polyclonal Tregs showing limited clinical efficacy. Promising pre-clinical results testing antigen-specific CAR Tregs [4] led to the first CAR Treg clinical trial authorization (NCT04817774) for kidney transplant patients, using *ex vivo,* autologous, naïve Tregs engineered with a CAR construct recognizing HLA-A2, to investigate the induction of tolerance in HLA-A2 negative patients receiving an HLA-A2 positive renal graft.

Currently, sourcing $CD4^+$ Teff and Tregs for cell therapies is invasive, time-consuming, and yields small numbers of cells, particularly of Tregs which comprise only 5-7% of the circulating CD4 T cell population [5]. Furthermore, $CD4^+$ Teff and Tregs obtained from these sources are polyclonal

56 in nature and can introduce variability and non-specificity. While we have been successful in
57 introducing a CAR construct in primary Tregs to mediate a specific immunosuppressive response
58 [4], the need to obtain antigen specific $CD4^+$ Teff and Tregs more efficiently and in large numbers
59 remains, especially genetically engineered Tregs.
60
61 Numerous studies have shown the ability to generate large quantities of T cells from iPSCs,
62 focusing primarily on the differentiation to cytotoxic T lymphocytes (CTLs) [6-8]. Improvements have
63 recently been made in the differentiation processes to generate iPSC-derived CAR CD8sp T cells
64 that more closely resemble primary $CD8\alpha\beta^+$ T cells rather than innate $\gamma\delta$ T cells, by knocking out
65 *TRAC* and delaying and attenuating CAR expression [9]. The artificial thymic organoid (ATO)
66 system has also proven to be successful in generating functionally mature $CD3^+CD8\alpha\beta^+$ T cells
67 that produce IFN-γ, TNF-α, and IL-2 and proliferate upon stimulation [8].
68
69 Interestingly, the ATO system also produces a small population of $CD3^+CD4^+$ T cells with a
70 conventional phenotype and diverse TCR repertoire [8, 10] that can be converted to $FOXP3^+$ Tregs
71 (Yano H. et al., ASH 2022). However, a scalable method to generate clinically relevant numbers
72 of $CD4^+$ T cells and Tregs from iPSCs has yet to be demonstrated. This need has become more
73 compelling in recent years as $CD4^+$ T effectors (Teffs) cells are known to enhance $CD8^+$ cytotoxic
74 T lymphocyte (CTLs) responses [11] and have been shown to be therapeutically useful in CAR-T
75 cell therapies increasing product potency [12, 13] and showing long-term functional persistency in
76 clinical trials [14].
77 Overall, current methods to generate CD8 single positive (CD8sp) T cells, CD4 single positive
78 (CD4sp) T cells and Tregs from iPSCs utilize serum or mouse stromal cells at some stage of the
79 differentiation process making it difficult for use in clinical development. In addition, the use of an
80 ATO system is challenging to scale-up for manufacturing as it requires the maintenance of a 3D

81 organoid system and involves dissociation and extraction of the cells of interest from a mixed
82 population of mouse and human cells. Here we show for the first time the ability to efficiently
83 generate both CD4sp T cells and Tregs from iPSCs in completely serum- and feeder-free
84 conditions. We identified a potent cell stimulator to convert $CD4^+CD8^+$ double positive T (DP T)
85 cells to CD4sp T cells at high efficiency that can then be converted to $FOXP3^+$ Tregs using TGFβ,
86 all-trans retinoic acid (ATRA), and IL-2 with CD3/CD28/CD2 activation. We show that the iPSC-
87 CD4sp T cells have an effector memory (T_{EM}) phenotype, are transcriptionally similar to primary
88 CD4 T conventional (Tconv) cells and can be activated upon stimulation. The iPSC-Tregs possess
89 typical Treg characteristics, are transcriptionally more similar to primary Tregs than primary Tconv
90 and suppress primary CD4 Tconv proliferation. In addition, iPSCs engineered to express an HLA-
91 A2 CAR and a fully functional TCR under the control of the *TRAC* promoter could effectively
92 differentiate to CD4sp T cells and then Tregs that also suppress Tconv proliferation *via* activation
93 through the TCR or HLA-A2 CAR. Finally, we also show that the iPSC-Tregs are amenable to
94 cryopreservation and retain function post-thaw. This novel method provides a viable path forward
95 towards the development of a scalable iPSC-derived Treg cell therapy and the development of
96 iPSC-derived CD4sp T cells which could enhance the iPSC-derived CD8sp T cell products
97 currently in the clinic for oncology applications [12, 14, 15].

98 ## Results

99 ### Generation of CD34$^+$ hematopoietic stem and progenitor cells (HSPCs) and T cell
100 progenitors from iPSCs

101 iPSC clones were derived from sorted CD4$^+$CD25$^+$ cells from a healthy human donor. Derivation
102 of iPSCs from T cells has been previously documented with resulting T cells differentiated from
103 reprogrammed iPSCs possessing antigen specificity due to retention of a rearranged TCR [7, 16, 17].
104 Additionally, evidence suggests improved T cell lineage differentiation when iPSCs originate from
105 mature T cells due to removal of the barrier to TCR rearrangement. [7, 18]. CD4$^+$CD25$^+$ T cells were
106 isolated and FACS-purified from healthy human leukapheresis blood and reprogrammed by
107 Sendai virus carrying vectors encoding for the four Yamanaka factors: OCT-4, SOX2, KLF4, and
108 C-MYC. Multiple clones were generated and characterized by immunocytochemistry to confirm
109 expression of OCT4, SOX2, TRA-1-81, and SSEA-4 **(Supp. Figure 1A)**. In addition, G-band
110 karyotyping confirmed the absence of any chromosomal aberrations **(Supp. Figure 1B)**.

111 To facilitate future translation from discovery to process development we utilized serum-free,
112 commercially available reagents from the iPSC stage to the DP T stage. As a first step, a modified
113 version of the spin embryoid body (EB) method was used to differentiate the iPSCs into early
114 stages of hematopoiesis from days 0 to 8, followed by expansion of the hematopoietic stem and
115 progenitor cells from days 8 to 14 [19, 20] **(Figure 1A)**. The EBs increased in size over time and by
116 day 14, numerous free-floating HSPCs emerged around the periphery expressing both CD34 and
117 CD45 (65%±13.5%, n=3) **(Figure 1B and 1C)**. The approximate yield of HSPCs per input iPSC
118 was 16.5±9.3, n=3 **(Figure 2)**.

119 For commitment and differentiation to the T cell lineage, interaction between blood cell progenitors
120 and a Notch ligand is required [21-23]. To differentiate the iPSC-HSPCs to lymphoid progenitors, the
121 entire population of free-floating HSPCs was separated from the EBs, collected, and seeded onto

122 plates coated with lymphoid differentiation coating material (LDCM), a commercially available
123 matrix containing a Notch ligand **(Figure 1D)**. The HSPCs were then further differentiated to
124 lymphoid progenitor cells that were CD5 and CD7 DP by day 28 (**Figure 1C**, 67.4±0.1%, n=6)
125 and subsequently to CD4 and CD8 DP T cells by day 42 (**Figure 1C**, DP T cells, 86.3±0.1%, n=5)
126 using a commercially available iPSC-HSPC to T cell differentiation system **(Figure 1D)**. The
127 approximate yield of lymphoid progenitor cells and DP T cells was 2.3e3±1.4e3 per input iPSC
128 and 2.6e4±1.6e4 per input iPSC, respectively **(Figure 2)**. We tested the use of CXCL12 (SDF1a)
129 and a p38 inhibitor (SB203580) to enhance the number of DP T cells [17] and found approximately
130 a 1.8-fold increase in DP T cells **(Supp. Figure 2)**.

131 **Generation of CD4-sp T cells and FOXP3$^+$ Tregs from iPSC-CD4$^+$CD8$^+$ DP T cells**

132 During T cell development in the thymus, TCR signaling is required in DP thymocytes to induce
133 positive selection and subsequent generation of either mature CD4$^+$ or CD8$^+$ T cells [24]. In addition
134 to differentiation into T cells, the interaction between the TCR and MHC molecules in the thymus
135 also rescues thymocytes from programmed cell death [25]. Alternatively, it has been shown that DP
136 thymocytes can undergo positive selection and maturation into CD4$^+$ T cells without engagement
137 of the TCR if provided with a strong, persistent signal [24, 26, 27]. We tested the ability of the iPSC-
138 derived DP T cells (iPSC-DP T) to convert to CD4sp T cells by exposure to three different doses
139 (low, medium, high) of the potent cell stimulator PMA/Ionomycin (PMA/I) **(Figure 3A).** A change
140 in phenotype was observed by 24 hours when the iPSC-DP T cells appeared to be primarily
141 CD8sp initially but shifted dramatically to become CD4sp 4 days after treatment. After 6 days,
142 more than 50% of the cells were CD4sp at the lowest concentration of PMA/I **(Figure 3B)**. Medium
143 to high concentrations of PMA/I were also effective in converting iPSC-DP T cells to CD4sp T
144 cells albeit at lower efficiency. The cells remained DP in the absence of PMA/I. Commitment to
145 the CD4 lineage is typically specified by the zinc-finger transcription factor and master regulator
146 ThPOK [28]. At the lowest concentration of PMA/I, ThPOK could be observed in the

147 $CD3^+TCR\alpha\beta^+CD4^+$ population of developing T cells **(Figure 3C)**. Without potent PMA/I
148 stimulation, the DP T cells did not progress towards the CD4 lineage and the minor population of
149 $CD4^+$ cells did not express ThPOK. The yield of CD4sp cells from PMA/I treated iPSC-DP T cells
150 was approximately 4.3e3±2.3e3/input iPSCs **(Figure 2)**. The generated iPSC-CD4sp cells
151 displayed a mostly T_{EM} phenotype ($CD45RO^+CD62L^-$) and highly expressed the co-receptor CD28
152 similar to primary CD4sp (**Figure 3D**).

153 After successfully generating bona fide CD4sp T cells from iPSCs, we next interrogated whether
154 a regulatory phenotype could be induced to produce Tregs. Previous studies have shown the
155 ability to generate $FOXP3^+$ Tregs from $CD4^+CD25^-$ T cells, termed induced Tregs (iTregs), in the
156 presence of TGFβ and IL-2 [29, 30 31]. To determine if the iPSC-CD4sp T cells could also be induced
157 to express FOXP3, cells were treated with a commercially available cocktail of TGFβ, all-trans
158 retinoic acid (ATRA), and IL-2 and supplemented with a soluble T cell activator composed of anti-
159 human CD3, CD28, and CD2 monospecific antibody complexes on day 50 of differentiation
160 **(Figure 3A)**. Seven days post-treatment (day 57) with the TGFβ cocktail and soluble activator, an
161 increase in frequency of DP and CD8sp T cells was observed and, while reduced, the culture
162 retained a sizeable CD4sp T cell population **(Figure 3E)**. When gating on the CD4sp T cell
163 population the cells expressed CD25, low levels of CD127 and high levels of FOXP3 similar to
164 primary Tregs. Approximately 26% (+/-9.2%; n=6) of the total live population displayed a ≥90%
165 CD4spCD25CD127lowFOXP3$^+$ phenotype. In addition, the CD4sp T cell population maintained
166 expression of ThPOK while co-expressing FOXP3 **(Figure 3E)**. We observed an average yield of
167 5.9e3±4.4e3 (n=3) iPSC-Treg/input iPSC **(Figure 2)**.

168 **iPSC-CD4sp T cells and iPSC-Tregs display a molecular signature similar to that of**
169 **primary CD4sp and Tregs respectively**

170 As the populations of iPSC-CD4sp cells and iPSC-Tregs are heterogenous post-PMA/I and post-
171 TGFβ and ATRA treatment, we sought to isolate the CD4sp population at day 50 and the target
172 Treg population of CD4spCD25^{+}CD127^{-}FOXP3^{+} iPSC-Tregs at day 57 by FACS to further
173 characterize them by single-cell RNA sequencing (scRNA-seq). For iPSC-Tregs, a population of
174 target cells that is >90% FOXP3 was obtained by gating on a "CD25 high" population from the
175 total population of live, single CD4sp T cells **(Supp Figure 3)**.

176 To determine the similarity between the iPSC-CD4sp to primary CD4 T cells and the iPSC-Tregs
177 to primary Tregs, their transcriptomes were compared. Four cell samples were analyzed: (1)
178 sorted iPSC-Tregs; (2) primary Tregs; (3) induced Tregs (generated from primary naïve CD4 T
179 cells); (4) iPSC-CD4sp; and (5) primary CD4 Tconvs. A global analysis of differentially expressed
180 genes by hierarchical clustering revealed that iPSC-CD4sp T cells were similar in their
181 transcriptional profile to primary Tconv while primary Tregs were similar to induced Tregs. The
182 iPSC-Tregs however, were distinct in their gene expression profile **(Figure 4A).** We sought a more
183 refined analysis and examined the expression of a core Treg gene signature in all samples [32-34]
184 **(Figure 4B**). We found that the iPSC-Tregs were similar to primary Tregs and induced Tregs with
185 some differences in gene expression. The iPSC-Tregs had upregulated expression of *FOXP3 and*
186 *CTLA4* and downregulated expression of *TNFRSF1B*. Within the core Treg gene signature, iPSC-
187 CD4 T cells were less similar to primary Tregs and more similar to primary Tconv. Both primary-
188 and iPSC-CD4sp T cells upregulated *ANK3* expression and downregulated *TNFRSF1B*
189 expression compared to all other populations. However, the iPSC-CD4sp T cells expressed
190 several genes at a much higher level than their primary counterpart (*VAV3, PTPRK, IKZF2,*
191 *HPGD, RBMS3*).

192 **Characterization and functional assessment of iPSC-CD4sp T cells and iPSC-Tregs**

193 Further characterization and functional assessment were performed on sorted iPSC-CD4sp T
194 cells and compared to their primary Tconv counterpart. iPSC-CD4sp T cells were activated with
195 CD3/CD28/CD2 soluble activator. After activation, cells increased their expression of activation
196 markers CD25 and PD-1 at 24 hours **(Supp. Figure 4A and Supp. Figure 4B)** and at 48 hours
197 **(Figure 5A and Figure 5B)** while decreasing expression of CD28 similar to Tconv **(Supp. Figure**
198 **4B and Figure 5B)**. While CD69 MFI increased after activation, the frequency of cells expressing
199 CD69 did not change. Activated iPSC-CD4sp T cells also secreted pro-inflammatory cytokines IL-
200 2 and TNF-α similar to activated primary Tconv but did not secrete IFN-γ. Similar levels of IL-4
201 and IL-10 were secreted by iPSC-CD4sp T cells compared to primary Tconv after stimulation
202 **(Figure 5C).**

203 We then characterized and examined the *in vitro* function of sorted iPSC-Tregs.
204 Immunophenotying of cells post-sort showed a typical Treg phenotype with an average of
205 83.4±6.3% FOXP3 expression (n=5) and average 91.6±1.6% Helios expression (n=2) from total
206 live cells. Demethylation of the evolutionarily conserved non-coding element FOXP3 Treg-
207 specific demethylated region (FOXP3 TSDR) is required for stable FOXP3 expression in Tregs [35].
208 It is typically methylated in Tconv, induced Tregs and other non-Treg blood cells [36]. We examined
209 the methylation state of FOXP3 TSDR by high resolution melt quantitative polymerase chain
210 reaction (HRM-qPCR) in the sorted iPSC-Tregs. The iPSC-Tregs demonstrated >90%
211 demethylation similar to the primary Treg positive control. In contrast, primary $CD4^{+}CD25^{-}$ Tconv
212 as well iPSC-CD4sp T cells were highly methylated at FOXP3 TSDR **(Figure 5D)**. The sorted
213 iPSC-Tregs could be activated via their TCR using beads coupled to anti-CD3 and anti-CD28
214 antibodies (Dynabeads). After activation, the iPSC-Tregs increased the expression of early
215 activation marker CD69 on average of 3-fold with no change to their Treg phenotype **(Figure 5E-**
216 **G)**.

217 Tregs typically exert their suppressive function through various mechanisms including
218 suppression by cytolysis [37, 38]. Cellular toxicity was determined by co-culturing activated and
219 unactivated iPSC-Tregs with primary CD4 Tconv target cells. Compared to activated cytotoxic
220 primary CD8 T cells, activated iPSC-Tregs had low cytolytic activity similar to activated primary
221 Tregs as measured by a LDH release assay **(Figure 6A).**

222 Additional suppressive mechanisms include secretion of anti-inflammatory cytokines like IL-10 [37].
223 IL-10 is produced by a variety of cells including $CD4^+$ Th2 cells, Tregs and IL-10-induced $CD4^+$ T
224 reg cells (Tr1 cells) [39]. Interestingly, iPSC-Tregs express higher, but variable, amounts of IL-10 as
225 compared to primary Tregs. Importantly, the iPSC-Tregs secreted low levels of pro-inflammatory
226 cytokines IL-2, IFN-γ, and TNF-α before and after activation, similar to primary Tregs **(Figure 6B)**.

227 The cardinal feature of Tregs is their ability to suppress the activation and proliferation of Tconv
228 or Teff cells by a cell-to-cell contact mechanism [37]. To determine the suppressive function of
229 activated iPSC-Tregs, the cells were co-cultured with activated primary Tconv and their
230 proliferation was measured by flow cytometric analysis. Activated iPSC-Tregs effectively
231 suppressed Tconv proliferation at a 1:1 ratio of Tregs:Tconv similar to activated primary Tregs
232 **(Figure 6C)**. Without activation, iPSC-Tregs had significantly lower levels of suppression at 1:1
233 to 1:4 Tregs: Tconv ratios. An iPSC-Treg dose-dependent effect on Tconv suppression was also
234 observed similar to primary Tregs. As expected, when iPSC-CD4sp T cells were tested for
235 suppressive function, they were unable to prevent Tconv proliferation even at the highest ratio of
236 1:1 CD4sp T cells:Tconv **(Figure 6C)**. This confirms that the suppressive function is specific to
237 iPSC-Tregs and appears only after conversion of iPSC-CD4sp T cells to $FOXP3^+$ Tregs and after
238 cell activation.

239 **Generation and functional assessment of HLA-A2 CAR^+ iPSC-Tregs**

240 We next investigated the function of iPSC-Tregs equipped with a chimeric antigen receptor (CAR).
241 To this end, we genetically engineered iPSCs to express an HLA-A2 CAR using zinc-finger
242 nucleases (ZFNs) targeting exon 2 of the *TRAC* gene.

243 We sought to retain expression of the *TRAC* gene and utilized a donor sequence comprised of
244 *TRAC* cDNA encompassing the *TRAC* exonic sequence downstream of the integration site. This
245 donor sequence is placed upstream and in-frame with a T2A coding sequence such that the
246 engineered locus retains expression of the TCRα chain while expressing an HLA-A2 CAR under
247 the control of the *TRAC* promoter **(Figure 7A)**. Through optimized electroporation of the iPSCs
248 with TRAC ZFN mRNA and donor DNA we achieved a >80% targeted integration without selection
249 as assessed by sequencing of the bulk edited population.

250 The resulting engineered iPSCs were cloned, expanded, and sequenced to obtain a biallelically
251 modified iPSC clone with the HLA-A2 CAR inserted at the target site. Sequencing analysis
252 confirmed the precise and in-frame insertion of a single copy of donor DNA (HLA-A2-CAR),
253 without any detected mutations. The CAR-engineered iPSCs also displayed a normal pluripotent
254 phenotype and were karyotypically normal **(Supp. Figure 1)**. To generate HLA-A2 CAR$^+$ iPSC-
255 Tregs (CAR iPSC-Tregs) the iPSCs were differentiated to HSPCs, lymphoid progenitor cells, and
256 DP T cells using the same differentiation process utilized for unedited iPSCs as described above
257 **(Supp. Figure 5A)**. HLA-A2 CAR iPSCs could also generate CD4sp T cells and FOXP3$^+$ Tregs
258 **(Supp. Figure 5B, 5C)**. Of note, we observed a 2.2-fold lower yield of Tregs (n=3, ±0.2 fold) from
259 the HLA-A2 CAR iPSCs compared to Tregs generated from unedited. By flow cytometric analysis,
260 we found that ~90% (90.1%±1.8%, n=4) of the DP T cells were already expressing the CAR by
261 day 42 and retained high CAR expression at both the CD4sp T cell (99%±0.2%, n=4) and Treg
262 stages (99.85%±0.1%, n=4). The intensity of CAR expression increased as the cells differentiated
263 as measured by MFI **(Supp. Figure 5D)**.

264 Similar to unedited iPSC-Tregs, HLA-A2 CAR$^+$ iPSC-Tregs could also be sorted. Four days post-
265 sort the expression levels of the CAR remained stable (81.3±12.4% of TCRαβ$^+$ cells and
266 MFI=9814.3±1143.3, n=3) and the cells maintained a high level of demethylation at FOXP3 TSDR
267 (88%±10.3%; n=3).

268 Further characterization showed that the CAR iPSC-Tregs could be activated through both the
269 TCR and the HLA-A2 CAR demonstrating the engineering strategy successfully retained TRAC
270 expression while integrating a functional CAR. Activation of the CAR iPSC-Tregs using either
271 CD3/CD28 beads (Dynabeads) or HLA-A2 dextramer upregulated CD69 expression compared to
272 unactivated or dextramer control activation **(Supp. Figure 6A, 6B)**. TCR- and CAR-mediated
273 activation induced a very low level of pro-inflammatory cytokines while inducing higher levels of
274 IL-10 **(Supp. Figure 6C)** similar to levels of cytokines produced by unedited iPSC-treg upon TCR
275 activation **(Figure 6B).** The CAR iPSC-Tregs significantly suppress Tconv proliferation at similar
276 levels to wild-type iPSC-Tregs when activated either through the TCR or the HLA-A2 CAR, while
277 unactivated or control dextramer activated CAR iPSC-Tregs only displayed a basal level of
278 suppression **(Figure 7B).**

279 Characterization and functional assessment of cryopreserved CAR iPSC-Tregs

280 A requirement for a viable CAR iPSC-Treg therapy is the ability to efficiently cryopreserve and
281 store the cells for future use without loss of stability and function. Towards that goal, we
282 cryopreserved iPSC-Tregs post-sort and then thawed, characterized, and tested their suppressive
283 function. Approximately 80% of cells were recovered post-thaw (avg=82.5%, n=2) with a viability
284 comparable to pre-cryopreservation (avg=74%, n=2). The CAR iPSC-Tregs maintained their
285 phenotype post-thaw **(Supp. Figure 7A)**. The cells were also highly demethylated at FOXP3
286 TSDR (95.5±0.5%, n=2) and displayed an average 4-fold increase in CD69 after activation *via*

287 the HLA-A2 CAR **(Supp. Figure 7B).** Finally, thawed CAR iPSC-Tregs were able to suppress

288 Tconv proliferation when activated *via* the TCR or CAR **(Figure 7C).**

289 **Discussion**

290 We report here for the first time a serum- and feeder-free method to produce CD4sp T cells and
291 functional Tregs with and without a CAR from iPSCs. While the generation of CD4sp T cells from
292 iPSCs has been reported [8, 10], it currently requires the use of murine stromal cells, animal serum
293 (fetal bovine serum, FBS) and ATOs. The use of xenogenic feeders, animal serum and 3D
294 organoids is not ideal for the development of a clinical-grade therapeutic product. This is due to
295 issues with safety, scalability and serum batch-to-batch heterogeneity as well as difficulty
296 dissociating cells from 3D organoids. In addition, automation of 3D organoid generation to
297 produce large-scale reproducible organoids is a nascent field and will require further optimization
298 to minimize variability across differentiation batches [40]. The method proposed here circumvents
299 many of these issues and increases its amenability for manufacturing cell therapies at scale.

300 The reprogramming of T cells to pluripotency and subsequent differentiation to mature T cells has
301 been well documented particularly towards the generation of CD8$\alpha\beta^+$ CTLs [41, 42 43]. Using T cell-
302 derived iPSCs may aid in more efficiently generating iPSC-T cells as the early stages of T cell
303 development that are characterized by failed TCR rearrangement and cell death are bypassed [44].
304 While antigen specificity is unknown, reprogramming from a T cell clone possessing a single TCR
305 [7, 16, 45] or introducing a CAR or transgenic TCR at the iPSC or T cell stage [6, 9, 17, 46-48] can help
306 confer specificity. Based on these findings, we sought to utilize a similar strategy to develop
307 CD4sp T cells and Tregs from iPSCs. We were able to successfully obtain iPSCs from mature
308 CD4sp T cells that expressed classic pluripotency markers and appeared as compact colonies
309 with well-defined borders. The iPSCs were amenable to genome engineering for the targeted
310 integration of an HLA-A2 CAR. Both the wild-type and engineered iPSC lines were karyotypically
311 normal **(Supp. Figure 1)**. We did not perform deep characterization of off-targets in edited iPSCs
312 at this research-grade stage. Most importantly, an advantage of using iPSCs over primary cells is

313 the ability to select through whole-genome sequencing (WGS) well-characterized clones with no
314 specific off-targets and expand them to generate a MCB for future clinical use.

315 Methods to differentiate iPSCs into HSPCs and progenitor T cells are readily available, but many
316 require the combination of multiple individual reagents from various sources which may contribute
317 to increased variability in differentiation. We found that utilizing commercially available reagents
318 specifically designed to generate HSPCs and T cell progenitors from iPSCs streamlined the
319 differentiation process while satisfying the serum- and feeder-free requirements. We utilized a
320 modified EB-based method to differentiate iPSCs and employed commercially available serum-
321 free media for the generation of $CD34^{+}CD45^{+}$ HSPCs capable of differentiation to lymphoid cells.
322 It is worth noting that while the process yielded a mixture of $CD34^{+}$ and $CD34^{-}$ cells, no enrichment
323 or purification for $CD34^{+}CD45^{+}$ target cells was required for further differentiation. Indeed, we
324 found that by separation of the free-floating progenitor cells from the main EB we were able to
325 generate lymphoid progenitor cells that co-expressed CD5 and CD7 marking their T cell
326 commitment [49, 50]. Continued differentiation of the lymphoid progenitor cells resulted in CD4 and
327 CD8 DP T cells again, without enrichment of the starting population.

328 Thymic DP T cells express both CD4 and CD8 co-receptors that promote TCR engagement of
329 MHC ligands to enhance signal transduction [24]. Through various strengths of binding affinity to
330 MHC ligands, the developing T cells will undergo positive selection to survive or cell death by
331 negative selection [51]. The step-by-step natural process followed by DP T cells after positive
332 selection to commit to either the CD4sp or CD8sp lineage is unclear. [24]. It has been suggested
333 that a persistent TCR signal is required to make the CD4 choice and block re-expression of the
334 CD8 co-receptor. To mimic the signal required for positive selection and commitment to the CD4
335 lineage at the DP T cell stage, we utilized a strategy previously shown to induce CD4 commitment
336 in murine DP T thymocytes without TCR engagement [26]. The addition of PMA/I activates protein
337 kinase c and elevates calcium levels, respectively and in a similar manner to TCR-mediated

338 activation with signals from co-stimulator molecules like CD4, CD8 and LFA-1 [26, 52]. At levels
339 between 0.016 uM to 0.16 uM of PMA and 0.13 uM of ionomycin, TRAC KO murine DP T
340 thymocytes are positively selected to CD4 T cells. Higher concentrations of PMA/I (1.6 uM and
341 1.3 uM, respectively) were inefficient in generating CD4 T cells. These findings are consistent with
342 our method in that the lower concentrations we used successfully converted cells to the CD4
343 lineage while higher concentrations of PMA/I were less efficient. Importantly, after conversion to
344 CD4sp T cells, ThPOK expression was observed further confirming its lineage commitment. The
345 kinetics of co-receptor expression in our system is different from what has been previously
346 published in mouse-derived thymocytes [26, 52, 53] and could be due to species-specific differences
347 between mouse and human thymocyte development [54], differences in the systems used (iPSC-
348 derived vs. thymus-derivates DP T cells) or related to the transient expansion of a highly
349 proliferative, immature intermediate ($CD4^-$ $CD8^+$ $Mki67^+$) [54]. Further characterization of the
350 intermediate stages will shed light on the mechanisms of PMA/I in our system.

351 Initial characterization of the iPSC-CD4sp T cells shows that they have a predominantly T_{EM}
352 phenotype, can be activated and secrete pro-inflammatory cytokines (IL-2 and TNF-α) upon
353 stimulation. However, we did not detect IFN-y from the iPSC-CD4sp T cells but observed IL-10
354 and IL-4 cytokines at similar levels to primary Tconv. The lack of IFN-y could suggest that the
355 iPSC-CDsp T cells are more similar to Th2 cells which are characterized by their secretion of IL-
356 4 and IL-10 and lack of IFN-y production when compared to Th1 cells [55 56] (Yano et al. ASH 2019).
357 Infusion of a defined CD4:CD8 CAR T cell ratio allows for a potentially more potent and
358 predictable product [12]. While some studies demonstrate that naive CD4sp CAR-T in combination
359 with CD8sp CAR T cells confer higher antitumor responses than T_{EM} CD4sp in *in vivo* mouse
360 models [13], others show potent antitumor activity using a mixture of naive and effector like CD4sp
361 CAR T cells in humans [12]. As the field matures to identify the characteristics of an ideal CD4sp
362 product, further optimization of our protocol can fine tune the final phenotype of our iPSC-CD4sp.

363 In addition to maintaining a serum- and feeder-free differentiation system, the use of PMA/I to
364 generate iPSC-CD4sp T cells is an especially critical finding as providing a positive selection
365 signal towards the CD4 lineage is the first step to generating Tregs. After maturation, the iPSC-
366 CD4sp T cells were treated with TGFβ, ATRA, IL-2 and a soluble CD3/CD28/CD2 activator to
367 convert them to a $FOXP3^+$ Treg phenotype. The generation of Tregs from naïve CD4 T cells using
368 TGFβ is well-documented [31]. While TGFβ-induced iTregs express FOXP3, they are only partially
369 demethylated at FOXP3 TSDR and are unstable in their expression of FOXP3. In addition,
370 polyclonal iTregs do not always display a regulatory phenotype, are not always suppressive and
371 can produce high levels of inflammatory cytokines [57]. In contrast, the iPSC-Tregs generated within
372 our system were highly demethylated at FOXP3 TSDR, suppressed Tconv proliferation and did
373 not produce inflammatory cytokines despite utilizing TGFβ towards its conversion. Transcriptomic
374 analysis by scRNA-sequencing further confirmed the identity and similarity of the iPSC Tregs to
375 primary Tregs. The iPSC-Tregs expressed typical markers of their primary natural Treg
376 counterpart, namely highly expressing *FOXP3*, *IKZF2* and *IL2RA* in the absence of activation.
377 The iPSC-Tregs also expressed a previously published core Treg signature [32-34] similar to that of
378 primary Tregs and less similar to iTregs and Tconv. Differential expression of genes between
379 iPSC-Treg and primary Treg, such as *IL7R* and *ID2*, could be due to culture conditions or to
380 differences between cells that differentiated *in vitro* as compared to *ex vivo* adult cells. Finally,
381 since scRNAseq utilizes relative expression levels, measuring the absolute expression of these
382 markers by bulk RNAseq may provide better quantitative results to distinguish these populations.

383 Previous studies have shown that iPSCs derived from T cells express TCRαβ prematurely which
384 interferes with DP T cell formation and can be overcome by supplying the cells with a strong Notch
385 signal [9]. Constitutive expression of CAR with simultaneous expression of the endogenous TCR,
386 however, offsets the effects of a stronger Notch signal. In this case, both elimination of TRAC
387 expression as well as attenuation of the CAR signal was required to restore DP T cell generation

388 [9]. These are important considerations for the generation of a scalable cell therapy product using
389 engineered iPSCs. While we were able to generate DP T cells from both wild-type and engineered
390 iPSCs, the exact Notch ligand in the LDCM reagent is unknown making the need to test a known
391 Notch ligand necessary for improving DP T cell yields. In addition, we observed a lower yield of
392 HLA-A2 CAR^+ iPSCs-Tregs as compared to Tregs generated from unedited iPSCs, supporting
393 the idea that premature TCR expression and CAR signaling influences DP T cell yields and
394 subsequent Treg generation. Defining the Notch ligand, optimizing CAR signaling as well as
395 applying compound-based measures to improve DP T cell yield from iPSCs can aid in the
396 generation of a more robust and reproducible differentiation protocol [9].

397 Cryopreservation is key to the development and delivery of successful cell therapy products. We
398 found that our CAR iPSC-Tregs were amenable to cryopreservation and showed similar viability
399 pre- and post-cryopreservation with approximately 80% recovery post-thaw. The phenotype of the
400 cells was also maintained pre- and post-thaw with appreciable upregulation of CD69 post-
401 activation via the CAR or TCR. Importantly, the cryopreserved iPSC-Tregs suppress Tconv
402 proliferation in vitro confirming that the cells maintain functionality **(Figure 7)**.

403 Further characterization of the iPSC-Tregs and iPSC-CD4sp T cells is still required, including
404 evaluation of its ability to expand to clinically relevant numbers and its function in a GvHD
405 mouse model. While additional data are essential to develop a viable cell therapy, we
406 demonstrated here a method to generate functional and stable iPSC-derived Tregs and CD4sp
407 T cells that removes the inconsistencies and safety issues caused by using xenogenic
408 materials. iPSCs can serve as an endless supply of CD4sp T cells and Tregs with and without a
409 CAR for therapeutic applications and our study supports further development of this process for
410 clinical use in oncology and autoimmune diseases.

411 ## Methods

412 **Generation of human induced pluripotent stem cell lines.** Previously cryopreserved CD4 T
413 cells were used for reprogramming to pluripotency. CD4 T cells were isolated from mobilized
414 leukapheresis material from a healthy male donor (AllCells, LLC) with informed written consent.
415 The raw material was washed several times to remove platelets, labeled with CD4 microbeads
416 (Miltenyi Biotec) and then isolated using the Miltenyi CliniMACS system. Isolated CD4 T cells
417 were analyzed for purity prior to cryopreservation. To prepare for reprogramming, the CD4 T cells
418 were thawed and cultured overnight in RPMI + 10% human AB serum (huABS, Valley Biomedical)
419 and activated 1:1 with CD3/CD28 Dynabeads in 100 U/mL of IL-2 (Thermofisher). The next day,
420 the CD4 T cells were debeaded and sorted for $CD4^{+}CD25^{+}$ cells and recovered overnight in RPMI
421 + 10% huABS with 100 U/mL of IL-2. One day post-sort, the sorted CD4 T cells were
422 reprogrammed with Sendai virus carrying the four transcription factors OCT, SOX2, KLF4, and C-
423 MYC as previously reported using Cytotune iPS-2.0 Sendai Reprogramming Kit (Thermofisher;
424 Fusaki Proc Japan Academy 2008). After transduction, cells were recovered in RPMI + 10%
425 huABS for 24 hours and transferred to ReproTeSR media (StemCell Technologies) on Matrigel-
426 coated plates (Corning). Cells were fed daily or every day until the appearance of colonies by day
427 14. Colonies were examined for appropriate morphology then manually selected for further
428 expansion and transition to mTeSR1 media (StemCell Technologies)

429 **Characterization of human induced pluripotent cells lines.** Immunocytochemical analysis for
430 pluripotency of iPSC lines was performed by washing cells in 1X PBS (Thermofisher), fixed in 4%
431 paraformaldehyde for 20 minutes at 4°C, and blocked in 10% normal goat or rabbit serum with
432 0.5% Triton X-100 (Sigma) in PBS. Immunocytochemical analysis was performed using primary
433 antibodies and corresponding AlexaFluor-conjugated secondary antibodies (Thermofisher). All
434 antibodies were diluted and used according to manufacturer's instructions. Cell nuclei were

435 counterstained with DAPI in some experiments [58]. Images were collected using an EVOS Cell
436 Imaging System (Thermofisher). Karyotype analyses were performed by Cell Line Genetics.

437 **iPSC culture and clonal expansion.** iPSCs were maintained on Matrigel (Corning) in mTeSR1
438 media according to manufacturer's instructions (StemCell Technologies). For passaging, iPSC
439 colonies were detached briefly with either Accutase and manually scraped or with Gentle Cell
440 Dissociation Reagent. Cells were routinely passaged at a 1:8-1:10 split ratio in the presence of Y-
441 27632 (ROCK inhibitor, Tocris) for the first day after passaging and removed for subsequent media
442 changes.

443 For clonal expansion of transfected iPSCs, a method of low-density passaging was used. After
444 electroporation, iPSCs were passaged at a low seeding density (1e3, 2.5e3, 5e3 cells per well of
445 a 6-well plate) such that a single iPSC would give rise to a single colony in a Matrigel-coated 6-
446 well plate. iPSC colonies were then manually picked and expanded individually. Tightly packed
447 colonies with clearly defined borders were then collected for genomic DNA isolation and
448 subsequent screening for targeted integration.

449 **Differentiation of HSPCs from iPSCs**. iPSCs were differentiated as previously described with
450 modifications [19, 20]. Embryoid bodies were generated from iPSCs in APEL2 media (StemCell
451 Technologies) and cultured in non-tissue culture or ultra-low attachment 96-well round bottom
452 plates in the presence of 10 ng/mL BMP4, 10 ng/mL VEGF, 50 ng/mL SCF, 10 ng/mL bFGF, and
453 10 uM Y-27632 on day 0 (all cytokines from Thermofisher). EBs were then cultured in APEL2
454 media in the presence of 20 ng/mL VEGF, 10 ng/mL bFGF, 100 ng/mL SCF, 20 ng/mL FLT-3L, 20
455 ng/mL TPO and 40 ng/mL IL-3 from day 1 to day 6 with a media refresh every 2 days (all cytokines
456 from Thermofisher). On day 8, EBs were switched to complete StemPro-34 media (Thermofisher)
457 and supplemented with 100 ng/mL SCF, 20 ng/mL FLT3-L, 20 ng/mL TPO, and 40 ng/mL IL-3 in
458 order to expand developing HSPCs. Media was refreshed every 2 days until day 14. The EBs

459 were then collected and passed through a 70 uM cell strainer. The resulting cell suspension
460 containing the HSPCs was then used for downstream differentiation.

461 **Differentiation of T cell progenitors from iPSC-HSPCs.** StemDiff T cell kit (StemCell
462 Technologies) was used to differentiate HSPCs to lymphoid progenitor cells and to DP T cells.
463 Manufacturer's instructions were followed unless otherwise indicated. HSPCs were seeded at
464 50,000 cells/well of a 6-well plate coated with lymphocyte differentiation coating material (LDCM)
465 and cultured in StemSpan Lymphoid Progenitor Expansion Media to differentiate the HSPCs to
466 CD5+CD7+ lymphoid progenitor cells. After 14 days of culture (differentiation day 28), resulting
467 iPSC-lymphoid progenitor cells were harvested and seeded at 0.5e6/well of a 6-well plate with a
468 fresh coating of LDCM. The cells were cultured in StemSpan T Cell Progenitor Maturation Media
469 (maturation media) for differentiation to CD4+CD8+ DP T cells. After 14 days of culture
470 (differentiation day 42), the DP T cells were harvested for further differentiation.

471 **Generation of CD4-single positive T cells and Tregs from iPSC-DP T cells.** Induction of DP
472 T cells to CD4sp T cells was performed on LDCM in maturation media. On differentiation day 42,
473 a cell stimulation cocktail composed of phorbol 12-myristate 13-acetate and ionomycin was added
474 to the cultures at three different concentrations from the 500X stock concentration: low (0.01 uM
475 PMA, 0.16 uM I), medium (0.02 PMA uM, 0.335 uM I), and high (0.0405 uM PMA, 0.67 uM I). A
476 full media change was performed 24 hours later by harvesting the entire cell suspension, replating
477 into fresh maturation media and seeding at a 1:1 ratio onto new LDCM coated 6-well plates. The
478 cells were then fed every 3-4 days for an additional week until day 50. On day 50, the cells were
479 then treated with 20 uL/mL of Immunocult Human Treg Differentiation Supplement (StemCell
480 Technologies) containing recombinant human TGF-B1 and all-trans retinoic acid, 12.5 uL/mL of
481 Immunocult Human CD3/CD28/CD2 T cell activator (StemCell Technologies) and 10 ng/mL of
482 CTS IL-2 (Thermofisher). Media in the wells for conversion to Tregs was composed of a 50%
483 mixture of complete CTS OpTmizer and maturation media. A half media change was performed

484 on day 54 with a 50% mixture of CTS OpTmizer and maturation media supplemented with 10
485 ng/mL of IL-2.

486 **Flow cytometry, sorting and antibodies.** Flow cytometry was performed in FACS buffer
487 composed of PBS, 0.5% BSA, and 1 mM EDTA. For extracellular staining, antibodies were added
488 to cells according to manufacturer's instructions, incubated at 4°C for 20 minutes, and washed
489 before analysis. For intracellular staining, cells were first stained with extracellular markers and
490 fixed and permeabilized using the eBioscience FOXP3/Transcription Factor Staining Buffer set
491 (Thermofisher). Antibodies were then added according to manufacturer's instructions. Attune NxT
492 flow cytometer (Thermofisher) and Sony Sorter SH800 was used for flow cytometric analysis and
493 sorting, respectively. Antibodies (clones in parentheses) used for surface and intracellular staining
494 of the following molecules were obtained from Biolegend: CD45 (HI30), FOXP3 (206D), ThPOK
495 (11H11A14), TCRab (IP26), Helios (22F6), and CD127 (A019D5). Antibodies against CD34 (581)
496 and CD3 (UCHT1) were obtained from BD Biosciences. Antibodies against CD4 (OKT-4), CD4
497 (VIT4), CD8 (SK1), FOXP3 (PCH101), CD69 (REA824), CD25 (2A3), CD28 (S20013F), CD45RA
498 (HI100), CD45RO (UCHL1), CD27 (O323), CD62L (DREG-56), and PD-1 (EH12.1) were obtained
499 from Thermofisher. CD5 (UCHT1) and CD7 (CD7-687) antibodies were obtained from Miltenyi.
500 Antibodies to SOX2, OCT4, SSEA-4 were obtained from R&D Systems. TRA-1–81 was obtained
501 from Santa Cruz Biotechnology. Alexa-conjugated secondary antibodies and DAPI were obtained
502 from Thermofisher.

503 **scRNA-sequencing RNA extraction, library generation, and sequencing analysis.** RNA from
504 iPSC-Tregs, iPSC-CD4sp, primary Tregs, induced Tregs and primary Tconv was extracted using
505 an RNA extraction kit (Qiagen) following differentiation (iPSC-Tregs and induced Tregs) or
506 isolation and culture (primary Tregs and Tconv).

507 Single cell RNA-sequencing libraries were sequenced on a NextSeq 500. Samples had an
508 average depth of 18636 reads per cell. Read quality control, UMI counting, barcode counting, and

509 alignment to the GRCh38 GENCODE v32/Ensembl 98 reference genome from 10x Genomics
510 were performed using the “cellranger 6.0.2” pipeline. All downstream analysis were performed
511 using the Seurat packages in R for single-cell RNAseq analysis.

512 All samples were filtered on the following measures: number of unique genes detected, total
513 number of molecules detected, and level of expression of mitochondrial reads before integrating
514 the datasets. We removed cells in which greater than 20% mitochondrial reads, less than 200
515 feature counts, or greater than 6500 feature counts were detected.

516 The data was then normalized using the Seurat normalization function which divides the feature
517 counts by total counts for each cell, then multiplies the resulting fraction by a scale factor of
518 1.00e+4, and, lastly, log-normalizes this value.

519 Dimensionality reduction was performed using Seurat packages and utilizing principal
520 components 1 through 50 in the reduction. Clusters were determined at a resolution of 0.3. The
521 identity of each cluster was validated by evaluation of gene expression within each cluster of cell-
522 type specific markers for the cell-types of interest.

523 **Assessment of iPSC-CD4sp T cell and iPSC-Treg Function.** For assessment of Tconv or iPSC-
524 CD4sp T cell phenotype and activation, cells were sorted and cultured in X-VIVO15 (Lonza) +
525 10% huABS (Valley Biomedical). Cells were either left unactivated or activated with Immunocult
526 Human CD3/CD28/CD2 T cell activator per manufacturer’s instructions (StemCell Technologies)
527 for 24 or 48hrs. Cells were then stained with indicated antibodies and run on flow cytometry as
528 previously described. For assessment of cytokine secretion, unactivated or activated iPSC-
529 CD4sp T cells were seeded at 5e4 cells/well in a round-bottom 96 well plate in 200 uL of media.
530 The supernatant was collected 24 hours later.

531 For assessment of iPSC-Treg function,cells were sorted on day 57 and cultured in complete
532 OpTmizer media supplemented with 1000U IL-2/mL (Thermofisher) for three days prior to

533 functional analysis. iPSC-Tregs were then activated with CD3/CD28 Dynabeads (Thermofisher)
534 at a ratio of 1:1 in media composed of X-VIVO15 (Lonza) + 10% huABS (Valley Biomedical) +
535 Penicillin / Streptomycin solution (pen/strep). For analysis of cytokine production, 5e4 activated
536 and unactivated cells were seeded in a round-bottom 96-well plate in 200 uL of media. One day
537 post-activation, supernatant was collected and analyzed for cytokines using human cytokine
538 assay X (Meso Scale Discovery). For assessment of Tconv suppression, activated and
539 unactivated iPSC-Tregs were co-cultured with activated (2:1 beads:cells) Tconv labeled with Cell
540 Trace Violet (Thermofisher) in X-VIVO15 media supplemented with pen/strep. iPSC-Tregs were
541 initially plated at 5e4/well in a 96-well round-bottom plate and serially diluted by a factor of 2 down
542 to 781.25 cells/well. 2.5e4 activated, CTV-labeled Tconv were then added to each serially diluted
543 well of iPSC-Tregs. Baseline Tconv proliferation was determined by culturing 2.5e4 Tconv in the
544 absence of iPSC-Tregs. Three days after co-culture, cells were collected, labeled for viability and
545 assessed for Tconv proliferation via Cell Trace Violet dye by flow cytometric analysis. For
546 assessment of iPSC-Treg cytolytic activity, activated and unactivated iPSC-Tregs were cocultured
547 with activated Tconv. 5e4 iPSC-Tregs were seeded with 5e4 primary Tconv and cultured for 3
548 days in X-VIVO15 media supplemented with pen/strep. The supernatant was then collected and
549 analyzed using the CyQuant LDH Cytotoxicity Kit (Thermofisher) following the manufacturer's
550 instructions. Samples were read on a SpectraMax microplate reader (Molecular Devices). Primary
551 Treg, Tconv and CD8 controls were cultured for 7-9 days prior to activation and assessment of
552 function.

553 **FOXP3 TSDR demethylation assay.** The Treg-specific demethylated region (TSDR)
554 hypomethylation status of FOXP3 gene was measured using a post-PCR High Resolution Melt
555 (HRM) analysis as previously described [4]. Briefly, genomic DNA was extracted from cell pellets
556 containing at least 1e6 cells/pellet using the DNeasy Blood and tissue kit (Qiagen), followed by
557 bisulfite conversion using the Epitech Fast Bisulfite Conversion Kit (Qiagen). The FOXP3 TSDR

558 regions were then amplified from the converted sample gDNAs by qPCR using specific primers
559 (forward: TTGGGTTAAGTTTGTTGTAGGATAG, reverse: ATCTAAACCCTATTATCACAACCCC,
560 Sigma Aldrich, USA) and Precision Melt Supermix (Biorad). The melting curves of amplified
561 product DNA fragments were quantified against the methylation standard curve generated using
562 commercial bisulfite converted human genomic DNAs (Qiagen) and expressed as a mean
563 methylation percentage.

564 **Cytokine MSD methods**. The concentrations of cytokines were measured with MSD U-Plex kits
565 (#K15067L-1, MSD, USA) following the manufacturer's protocol. Briefly, biotinylated capture
566 antibodies were incubated with specific linkers and then the mixture of linker coupled antibodies
567 was added to MSD U-Plex plates. After 1 hour incubation and wash step, standard curves and
568 samples were added to the plates. The plates were washed again after the sample incubation. A
569 mixture of SULFO-Tag conjugated detection antibodies was added to the wells and incubated.
570 After the final wash step, MSD GOLD Read Buffer B was added to the plate followed by reading
571 the electrochemiluminescence signals in a MESO SECTOR S 600 instrument.

572 **ZFN and donor DNA constructs**. The zinc finger nuclease (ZFN) pair targets the *TRAC* locus,
573 encoding for the alpha chain of the TCR, at exon 2. The ZFP backbone and FokI variants were
574 generated by reassembling zinc finger arrays from modules as previously described [59] and cloning
575 the resulting zinc finger array into a vector containing the desired FokI variant. All constructs were
576 verified by Sanger sequencing with two sequencing primers to yield overlapping sequence reads
577 of the entire ZFN coding sequence [60]. mRNA was transcribed from a PCR template using the 5×m
578 Message mMachine T7 ULTRA kit (Invitrogen) according to the manufacturer's instructions as
579 previously reported [60].

580 We designed and cloned the donor DNA sequence into a customized AAV vector containing AAV
581 inverted terminal repeats (ITRs). An AAV vector was initially selected to use AAV as DNA delivery
582 system but we ultimately optimized delivery using single strand DNA. The pAAV-partial-TRAC-

583 HLA-A2 CAR contains 110bp of genomic partial TRAC sequence (amplified by PCR) flanking the
584 TRAC homologous donor templates in frame with the second exon of TRAC, followed by a self-
585 cleaving T2A peptide, the HLA-A2 CAR and a bGHpA sequence.

586 **Transfection of TRAC-ZFN mRNA and donor DNA**. All transfections were performed on the
587 Maxcyte ATx (model GT) electroporation system. Approximately 3e6 iPSCs were used for
588 electroporation in an OC-100 processing assembly (Maxcyte). iPSCs were treated with Accutase
589 until cells were fully detached (~3min). After collection, cells were pelleted and washed once with
590 Maxcyte electroporation buffer. The iPSCs were then resuspended in Maxcyte electroporation
591 buffer at a concentration of 30e6 cells/mL and mixed with ZFN mRNA (10 ng/ul) and 8 ug of donor
592 DNA. The cell and nucleic acid mixture was dispensed into the OC-100 assembly and immediately
593 placed into the Maxcyte instrument using Optimization program 9. iPSCs were then recovered for
594 20 minutes at 37°C in the assembly and then transferred to Matrigel-coated plates in mTeSR1
595 media. Y-27632 was added to the media for 2-3 days post-transduction until confluent and then
596 passaged for clonal expansion.

597 **Analysis of targeted integration in iPSCs.** iPSCs were assessed quantitatively for on-target
598 insertions/deletions and targeted integration through NGS sequencing on the Illumina platform.
599 Genomic DNA from clonally expanded iPSCs was first amplified, followed by nested PCR
600 amplification to prepare ~200 bp amplicons for paired-end deep sequencing on the Illumina MiSeq
601 sequencer.

602 **iPSC-Treg Cryopreservation.** Post-sort CAR iPSC-Tregs were recovered in complete OpTmizer
603 supplemented with 1000U IL-2/mL at a concentration of 1e6/mL. 24 hours after recovery, CAR
604 iPS-Tregs were harvested, counted and cryopreserved in CryoStor CS10 (Biolife Solutions) at a
605 concentration of 4-5e6/mL. Cryopreserved cells were placed in an alcohol-free freezing container
606 (CoolCell, Corning) and placed at -80C overnight before transferring to LN2 for long-term storage.

607 **References**

608 1. Themeli, M., Riviere, I. & Sadelain, M. New cell sources for T cell engineering and
609 adoptive immunotherapy. *Cell Stem Cell* **16**, 357-366 (2015).

610 2. Dominguez-Villar, M. & Hafler, D.A. Regulatory T cells in autoimmune disease. *Nat*
611 *Immunol* **19**, 665-673 (2018).

612 3. Sanders, J.M., Jeyamogan, S., Mathew, J.M. & Leventhal, J.R. Foxp3+ regulatory T cell
613 therapy for tolerance in autoimmunity and solid organ transplantation. *Front Immunol* **13**,
614 1055466 (2022).

615 4. Proics, E. et al. Preclinical assessment of antigen-specific chimeric antigen receptor
616 regulatory T cells for use in solid organ transplantation. *Gene Ther* **30**, 309-322 (2023).

617 5. Raffin, C., Vo, L.T. & Bluestone, J.A. T(reg) cell-based therapies: challenges and
618 perspectives. *Nat Rev Immunol* **20**, 158-172 (2020).

619 6. Themeli, M. et al. Generation of tumor-targeted human T lymphocytes from induced
620 pluripotent stem cells for cancer therapy. *Nat Biotechnol* **31**, 928-933 (2013).

621 7. Nishimura, T. et al. Generation of rejuvenated antigen-specific T cells by reprogramming
622 to pluripotency and redifferentiation. *Cell Stem Cell* **12**, 114-126 (2013).

623 8. Montel-Hagen, A. et al. Organoid-Induced Differentiation of Conventional T Cells from
624 Human Pluripotent Stem Cells. *Cell Stem Cell* **24**, 376-389 e378 (2019).

625 9. van der Stegen, S.J.C. et al. Generation of T-cell-receptor-negative CD8ab-positive CAR
626 T cells from T-cell-derived induced pluripotent stem cells. *Nature biomedical engineering*
627 (2022).

628 10. Wang, Z. et al. 3D-organoid culture supports differentiation of human CAR(+) iPSCs into
629 highly functional CAR T cells. *Cell Stem Cell* **29**, 515-527 e518 (2022).

630 11. Borst, J., Ahrends, T., Babala, N., Melief, C.J.M. & Kastenmüller, K. CD4+ T cell help in
631 cancer immunology and immunotherapy. *Nature Reviews Immunology* **18**, 635-647
632 (2018).

633 12. Turtle, C.J. et al. CD19 CAR-T cells of defined CD4+:CD8+ composition in adult B cell
634 ALL patients. *J Clin Invest* **126**, 2123-2138 (2016).

635 13. Sommermeyer, D. et al. Chimeric antigen receptor-modified T cells derived from defined
636 CD8+ and CD4+ subsets confer superior antitumor reactivity in vivo. *Leukemia* **30**, 492-
637 500 (2016).

638 14. Melenhorst, J.J. et al. Decade-long leukaemia remissions with persistence of CD4+ CAR
639 T cells. *Nature* **602**, 503-509 (2022).

640 15. Tay, R.E., Richardson, E.K. & Toh, H.C. Revisiting the role of CD4(+) T cells in cancer
641 immunotherapy-new insights into old paradigms. *Cancer Gene Ther* **28**, 5-17 (2021).

642 16. Vizcardo, R. et al. Regeneration of human tumor antigen-specific T cells from iPSCs
643 derived from mature CD8(+) T cells. *Cell Stem Cell* **12**, 31-36 (2013).

644 17. Iriguchi, S. et al. A clinically applicable and scalable method to regenerate T-cells from
645 iPSCs for off-the-shelf T-cell immunotherapy. *Nature communications* **12**, 430 (2021).

646 18. Chang, C.W., Lai, Y.S., Lamb, L.S., Jr. & Townes, T.M. Broad T-cell receptor repertoire in
647 T-lymphocytes derived from human induced pluripotent stem cells. *PLoS One* **9**, e97335
648 (2014).

649 19. Ng, E.S., Davis, R., Stanley, E.G. & Elefanty, A.G. A protocol describing the use of a
650 recombinant protein-based, animal product-free medium (APEL) for human embryonic
651 stem cell differentiation as spin embryoid bodies. *Nat Protoc* **3**, 768-776 (2008).

652 20. Kotini, A.G. et al. Stage-Specific Human Induced Pluripotent Stem Cells Map the
653 Progression of Myeloid Transformation to Transplantable Leukemia. *Cell Stem Cell* **20**,
654 315-328 e317 (2017).

655 21. Schmitt, T.M., Ciofani, M., Petrie, H.T. & Zuniga-Pflucker, J.C. Maintenance of T cell
656 specification and differentiation requires recurrent notch receptor-ligand interactions. *J*
657 *Exp Med* **200**, 469-479 (2004).

658 22. Trotman-Grant, A.C. et al. DL4-mubeads induce T cell lineage differentiation from stem
659 cells in a stromal cell-free system. *Nat Commun* **12**, 5023 (2021).

660 23. Mohtashami, M., Brauer, P.M. & Zuniga-Pflucker, J.C. Induction of Human T Cell
661 Development In Vitro with OP9-DL4-7FS Cells Expressing Human Cytokines. *Methods*
662 *Mol Biol* **2580**, 249-260 (2023).

663 24. Singer, A., Adoro, S. & Park, J.H. Lineage fate and intense debate: myths, models and
664 mechanisms of CD4- versus CD8-lineage choice. *Nat Rev Immunol* **8**, 788-801 (2008).

665 25. Jameson, S.C., Hogquist, K.A. & Bevan, M.J. Positive selection of thymocytes. *Annu*
666 *Rev Immunol* **13**, 93-126 (1995).

667 26. Ohoka, Y. et al. In vitro differentiation and commitment of CD4+ CD8+ thymocytes to the
668 CD4 lineage, without TCR engagement. *Int Immunol* **8**, 297-306 (1996).

669 27. Takahama, Y., Suzuki, H., Katz, K.S., Grusby, M.J. & Singer, A. Positive selection of
670 CD4+ T cells by TCR ligation without aggregation even in the absence of MHC. *Nature*
671 **371**, 67-70 (1994).

672 28. Park, J.H. et al. Signaling by intrathymic cytokines, not T cell antigen receptors, specifies
673 CD8 lineage choice and promotes the differentiation of cytotoxic-lineage T cells. *Nat*
674 *Immunol* **11**, 257-264 (2010).

675 29. Fu, S. et al. TGF-beta induces Foxp3 + T-regulatory cells from CD4 + CD25 -
676 precursors. *Am J Transplant* **4**, 1614-1627 (2004).

677 30. Chen, W. et al. Conversion of peripheral CD4+CD25- naive T cells to CD4+CD25+
678 regulatory T cells by TGF-beta induction of transcription factor Foxp3. *J Exp Med* **198**,
679 1875-1886 (2003).

680 31. Mitsuhiro, K., Hiroko, N., Masahiro, O., Qianjin, L. & Akihiko, Y. Induced Regulatory T
681 Cells: Their Development, Stability, and Applications. *Trends in Immunology* **37**, 803-811
682 (2016).

683 32. Pesenacker, A.M. et al. Treg gene signatures predict and measure type 1 diabetes
684 trajectory. *JCI Insight* **4** (2019).

685 33. Pesenacker, A.M. et al. A Regulatory T-Cell Gene Signature Is a Specific and Sensitive
686 Biomarker to Identify Children With New-Onset Type 1 Diabetes. *Diabetes* **65**, 1031-
687 1039 (2016).

688 34. Höllbacher, B. et al. Transcriptomic Profiling of Human Effector and Regulatory T Cell
689 Subsets Identifies Predictive Population Signatures. *ImmunoHorizons* **4**, 585-596 (2020).

690 35. Huehn, J., Polansky, J.K. & Hamann, A. Epigenetic control of FOXP3 expression: the
691 key to a stable regulatory T-cell lineage? *Nat Rev Immunol* **9**, 83-89 (2009).

692 36. Floess, S. et al. Epigenetic control of the foxp3 locus in regulatory T cells. *PLoS Biol* **5**,
693 e38 (2007).

694 37. Dikiy, S. & Rudensky, A.Y. Principles of regulatory T cell function. *Immunity* **56**, 240-255
695 (2023).

696 38. Vignali, D.A., Collison, L.W. & Workman, C.J. How regulatory T cells work. *Nat Rev*
697 *Immunol* **8**, 523-532 (2008).

698 39. Moore, K.W., de Waal Malefyt, R., Coffman, R.L. & O'Garra, A. Interleukin-10 and the
699 interleukin-10 receptor. *Annu Rev Immunol* **19**, 683-765 (2001).

700 40. Louey, A., Hernandez, D., Pebay, A. & Daniszewski, M. Automation of Organoid
701 Cultures: Current Protocols and Applications. *SLAS Discov* **26**, 1138-1147 (2021).

702 41. Seki, T. et al. Generation of induced pluripotent stem cells from human terminally
703 differentiated circulating T cells. *Cell Stem Cell* **7**, 11-14 (2010).

704 42. Loh, Y.H. et al. Reprogramming of T cells from human peripheral blood. *Cell Stem Cell* **7**,
705 15-19 (2010).

706 43. Brown, M.E. et al. Derivation of induced pluripotent stem cells from human peripheral
707 blood T lymphocytes. *PLoS One* **5**, e11373 (2010).

708 44. Hernandez, J.B., Newton, R.H. & Walsh, C.M. Life and death in the thymus--cell death
709 signaling during T cell development. *Curr Opin Cell Biol* **22**, 865-871 (2010).

710 45. Nagano, S. et al. High Frequency Production of T Cell-Derived iPSC Clones Capable of
711 Generating Potent Cytotoxic T Cells. *Mol Ther Methods Clin Dev* **16**, 126-135 (2020).

712 46. Kawamoto, H., Masuda, K. & Nagano, S. Regeneration of antigen-specific T cells by
713 using induced pluripotent stem cell (iPSC) technology. *Int Immunol* **33**, 827-833 (2021).

714 47. Maeda, T. et al. Regeneration of Tumor-Antigen-Specific Cytotoxic T Lymphocytes from
715 iPSCs Transduced with Exogenous TCR Genes. *Mol Ther Methods Clin Dev* **19**, 250-
716 260 (2020).

717 48. Li, S. et al. Strength of CAR signaling determines T cell versus ILC differentiation from
718 pluripotent stem cells. *Cell Rep* **42**, 112241 (2023).

719 49. Awong, G. et al. Human proT-cells generated in vitro facilitate hematopoietic stem cell-
720 derived T-lymphopoiesis in vivo and restore thymic architecture. *Blood* **122**, 4210-4219
721 (2013).

722 50. Edgar, J.M., Michaels, Y.S. & Zandstra, P.W. Multi-objective optimization reveals time-
723 and dose-dependent inflammatory cytokine-mediated regulation of human stem cell
724 derived T-cell development. *NPJ Regen Med* **7**, 11 (2022).

725 51. Klein, L., Robey, E.A. & Hsieh, C.S. Central CD4(+) T cell tolerance: deletion versus
726 regulatory T cell differentiation. *Nat Rev Immunol* **19**, 7-18 (2019).

727 52. Takahama, Y. & Nakauchi, H. Phorbol ester and calcium ionophore can replace TCR
728 signals that induce positive selection of CD4 T cells. *The Journal of Immunology* **157**,
729 1508-1513 (1996).

730 53. Karimi, M.M. et al. The order and logic of CD4 versus CD8 lineage choice and
731 differentiation in mouse thymus. *Nat Commun* **12**, 99 (2021).

732 54. Li, Y. et al. Development of double-positive thymocytes at single-cell resolution. *Genome*
733 *Med* **13**, 49 (2021).

734 55. Theofilopoulos, A.N., Koundouris, S., Kono, D.H. & Lawson, B.R. The role of IFN-
735 gamma in systemic lupus erythematosus: a challenge to the Th1/Th2 paradigm in
736 autoimmunity. *Arthritis Res* **3**, 136-141 (2001).

737 56. Butcher, M.J. & Zhu, J. Recent advances in understanding the Th1/Th2 effector choice.
738 *Fac Rev* **10**, 30 (2021).

739 57. Tran, D.Q., Ramsey, H. & Shevach, E.M. Induction of FOXP3 expression in naive human
740 CD4+FOXP3 T cells by T-cell receptor stimulation is transforming growth factor-beta
741 dependent but does not confer a regulatory phenotype. *Blood* **110**, 2983-2990 (2007).

742 58. Fong, H. et al. Genetic correction of tauopathy phenotypes in neurons derived from
743 human induced pluripotent stem cells. *Stem Cell Reports* **1**, 226-234 (2013).

744 59. Paschon, D.E. et al. Diversifying the structure of zinc finger nucleases for high-precision
745 genome editing. *Nat Commun* **10**, 1133 (2019).

746 60. Miller, J.C. et al. Enhancing gene editing specificity by attenuating DNA cleavage
747 kinetics. *Nat Biotechnol* **37**, 945-952 (2019).

748

749 **Acknowledgements.** We thank Prof. Maria Themeli for critical review of the manuscript and for
750 giving critical advice for our research work. We also thank Prof. Megan Levings for critical advice
751 on the transcriptomics analysis; Dr. Andreas Reik, Dr. Lei Zhang and Dr. George Kwong for
752 technical assistance; Dr. Julie Gertner-Dardenne, Dr. Maurus de la Rosa, Dr. David Fenard, Dr.
753 Tobias Abel and Dr. Virginie Fabre for scientific discussions; Mrs. Cayla McEwen and Mrs. Jean
754 Alladin for administrative support.

755

756 **Patents.** Part of this research work is described in the following patents:

757 US Patent number 11512287: “Targeted disruption of T cell and/or HLA receptors”

Application PCT/US2021/057152 (Filed Oct 28, 2021): “Generation of CD4+ Effector and Regulatory T cells from Human Pluripotent Stem Cells”

Application PCT/US2020/059730 (Filed Sep 11, 2020): “Generation of Engineered Regulatory T cells”

Author contributions. H.F., M.M., L.N., G.L., S.G., A.C. and S.Z. designed the study; H.F., M.M., J.J., L.N., K.K., S.S., J.H. and A.V. performed the experiments; H.F., M.M., J.J., L.N., K.K., G.L., S.G., S.S., J.H. and A.V. analyzed the data; H.F., M.M., L.N., S.S., A.C., J.F. and S.Z. interpreted the data; J.F. provided advice for the experiments; A.C. and S.Z. supervised the study; H.F. and S.Z. wrote the manuscript

Competing interests. All authors are current or former Sangamo Therapeutics employees and shareholders.

Correspondence and requests for materials should be addressed to H.F. and S.Z.

MAIN FIGURES

FIGURE 1. Differentiation of iPSCs to HSPCs, lymphoid progenitors and DP T cells in serum- and feeder-free conditions.

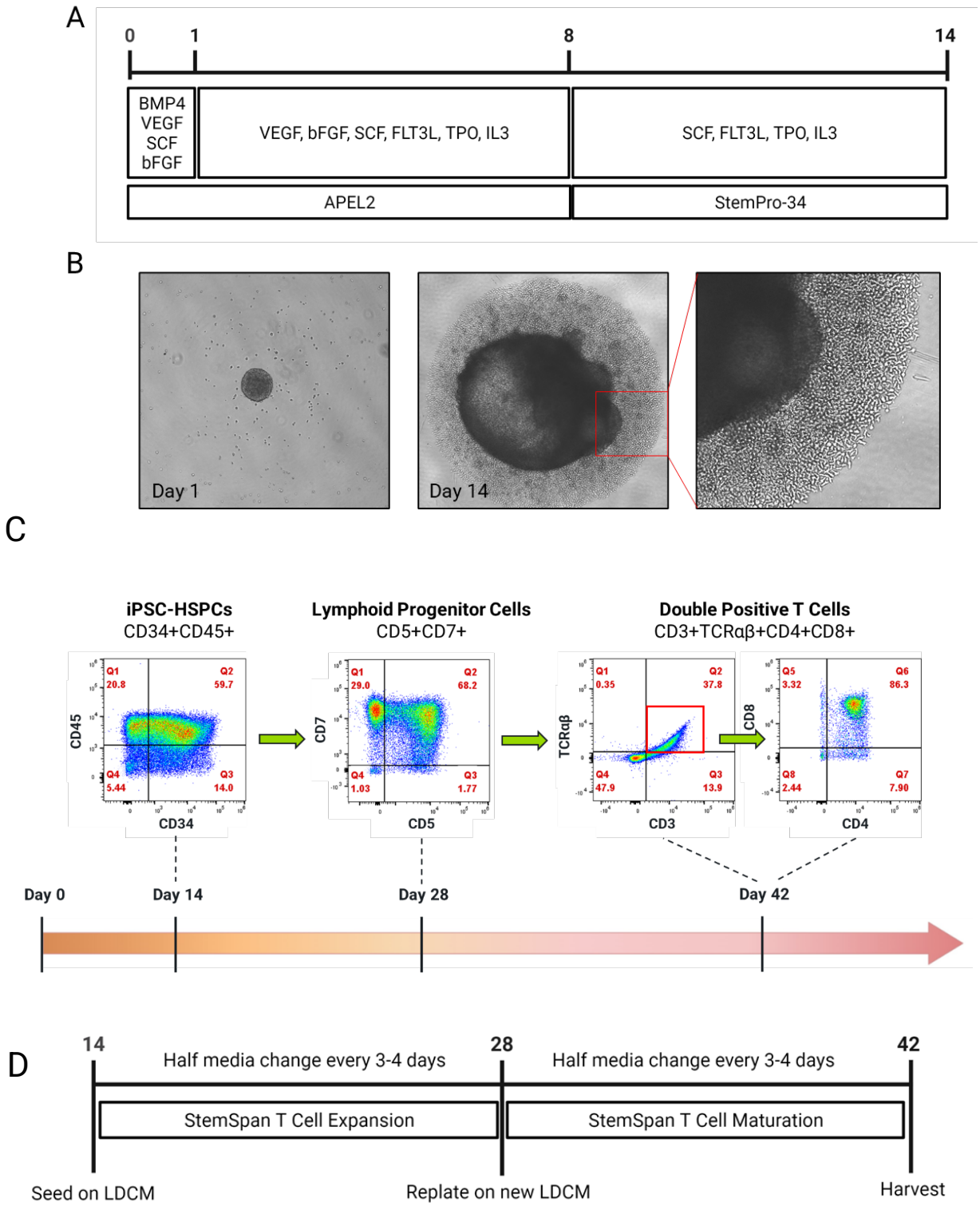

Figure 1. Differentiation of iPSCs to hematopoietic stem and progenitor cells (HSPCs), lymphoid progenitors and double positive (DP) T cells in serum- and feeder-free conditions.

A. Schematic for differentiation of iPSCs to HPSCs.
B. Embryoid bodies (EBs) at day 1 and 14 of differentiation. HSPCs emerged from the EB by day 14 and appeared as loosely packed cells (inset).
C. Representative flow cytometric analyses of HSPCs, lymphoid progenitor cells, and DP T cells from iPSCs. Cells were analyzed for phenotype over a 42-day period at the indicated timepoints (n=3).
D. Schematic for differentiation of iPSC-HSPCs to lymphoid progenitor cells and DP T cells.

FIGURE 2. Cell Yield per Input iPSC.

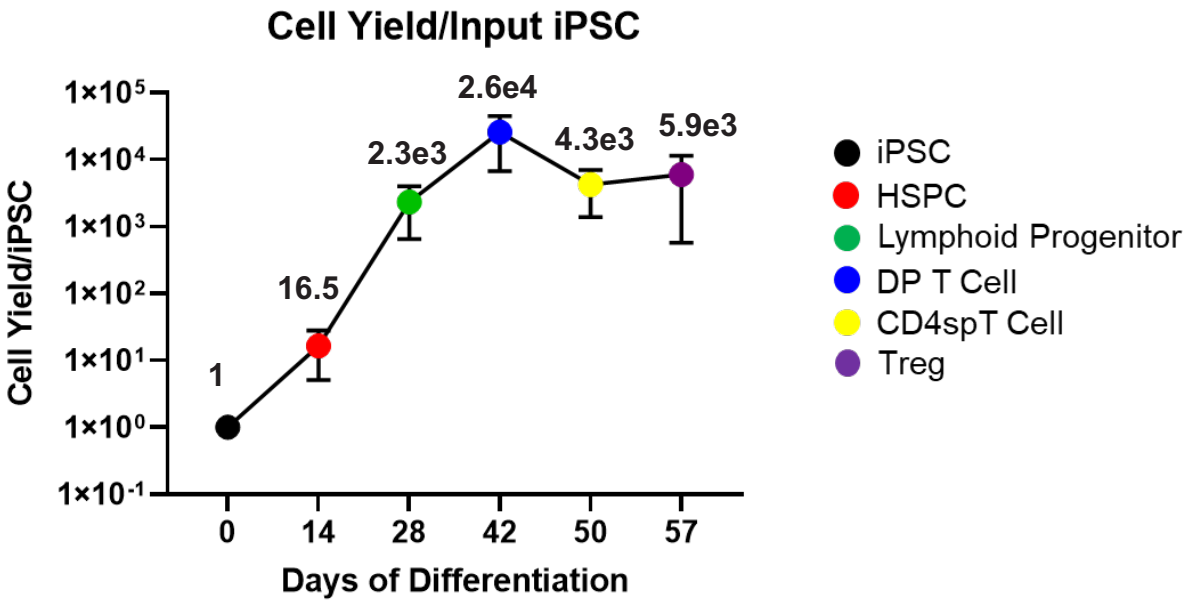

Figure 2. Yield of iPSC-derived hematopoietic stem and progenitor cells (HSPCs), lymphoid progenitors, double positive (DP) T cells, CD4sp T cells, and Tregs. Cell yield per input iPSC at various stages of differentiation (n=3).

FIGURE 3. Differentiation of iPSCs to CD4sp T cells and Tregs in serum- and feeder-free conditions.

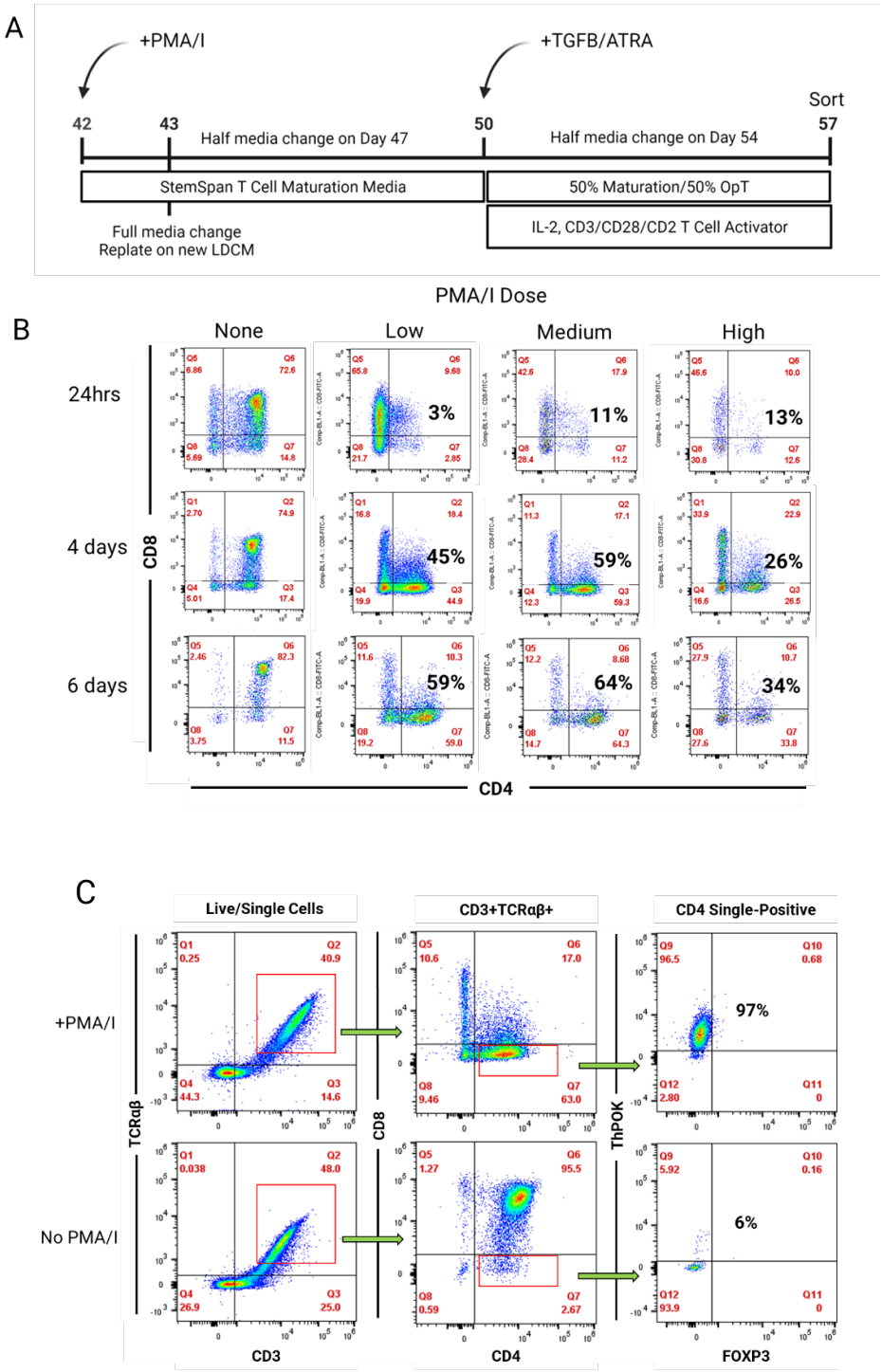

D

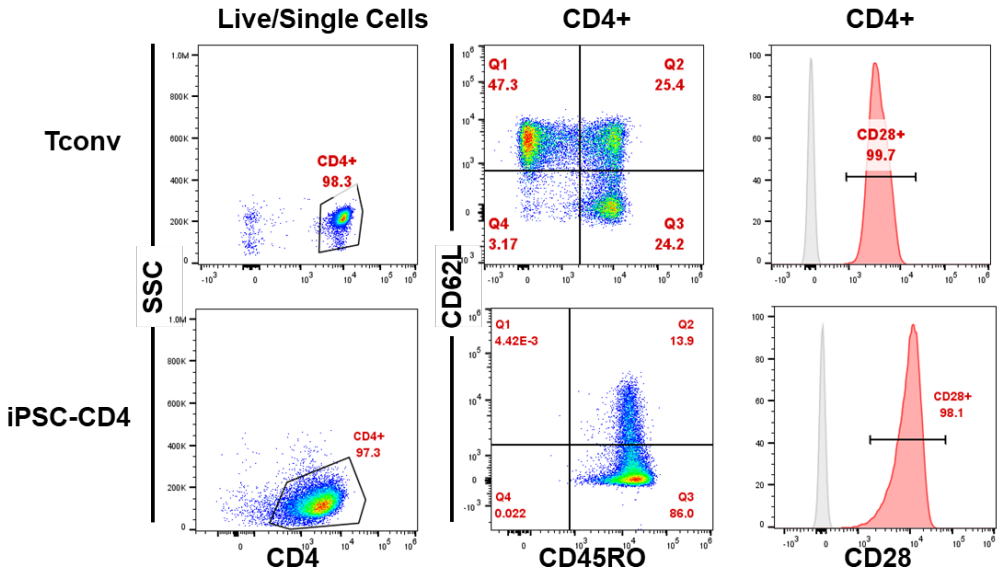
Live/Single Cells
CD4+
CD4+
Tconv
iPSC-CD4
SSC
CD4
CD4+
98.3
CD4+
97.3
CD62L
CD45RO
Q1
47.3
Q2
25.4
Q4
3.17
Q3
24.2
Q1
4.42E-3
Q2
13.9
Q4
0.022
Q3
86.0
CD28
CD28+
99.7
CD28+
98.1

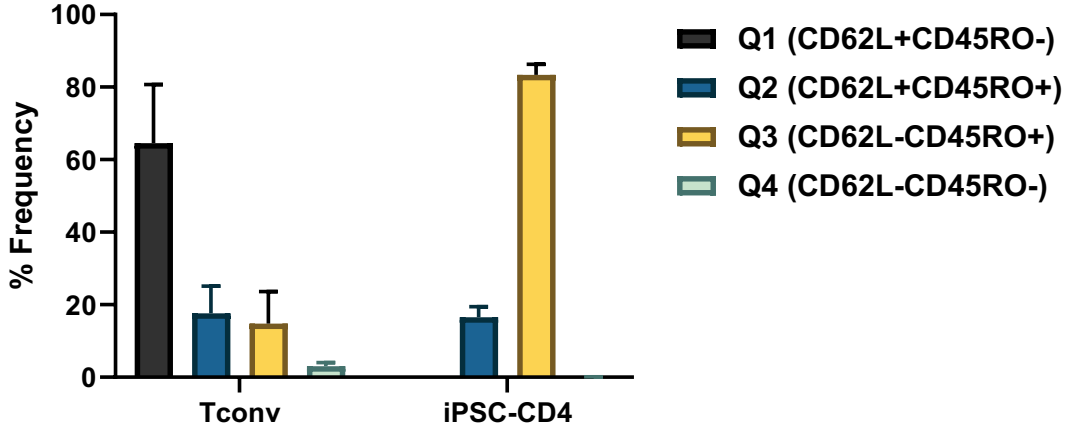
% Frequency
100
80
60
40
20
0
Tconv
iPSC-CD4
Q1 (CD62L+CD45RO-)
Q2 (CD62L+CD45RO+)
Q3 (CD62L-CD45RO+)
Q4 (CD62L-CD45RO-)

E

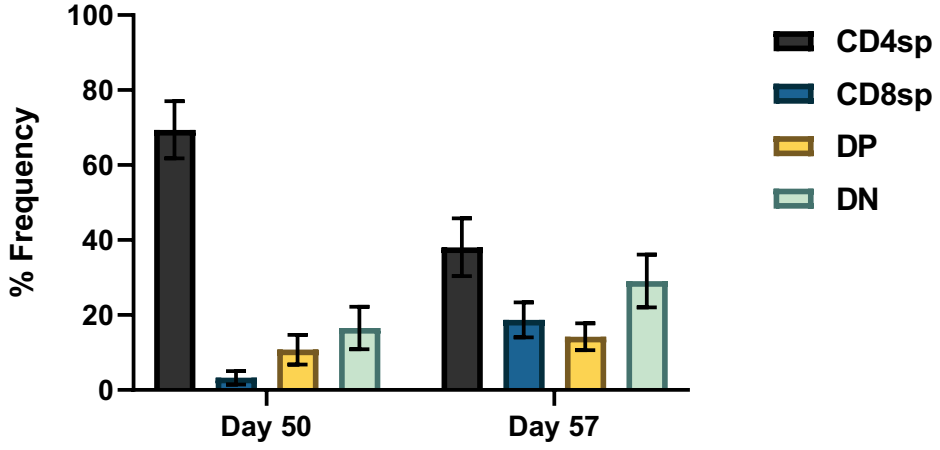
% Frequency
100
80
60
40
20
0
Day 50
Day 57
CD4sp
CD8sp
DP
DN

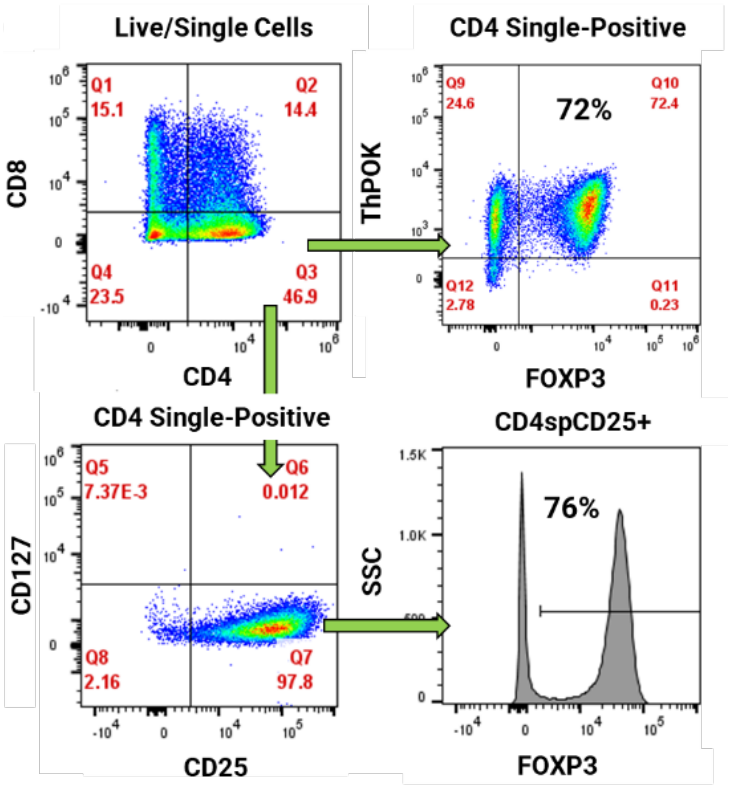

Figure 3. Differentiation of iPSCs to CD4sp T cells and Tregs in serum- and feeder-free conditions.

A. Schematic for differentiation of iPSCs to CD4sp T cells and Tregs.
B. Representative kinetic analysis of developing CD4sp T cells after Phorbol 12-myristate 13-acetate and Ionomycin (PMA/I) addition. Phenotype was assessed by the expression levels of CD4 and CD8 by flow cytometry.
C. Representative flow plots of iPSC-CD4sp T cells 8 days after PMA/I addition (day 50 of differentiation) to assess for CD4 commitment. Phenotype was assessed by the expression levels of CD3, TCRαβ, CD4, CD8, FOXP3 and ThPOK in cells with and without PMA/I treatment (n=6).
D. Representative flow plots and expression of CD4 markers in unactivated T conventional (Tconv)–and sorted unactivated iPSC-CD4sp T cells. Phenotype was assessed by flow cytometric analysis (n=3) in Tconv and iPSC-CD4sp at day 50 of differentiation for the expression of CD4, CD62L, CD45RO and CD28. CD28 FMO control (gray) and CD28 expression (red).
E. Frequency of cell subpopulations from all live cells at day 50 and day 57 of differentiation (top) and representative flow cytometric plots of iPSC-Tregs 7 days after TGFβ+ATRA addition (day 57 of differentiation) (bottom). CD4sp, CD8sp, double positive (DP), and double negative (DN) populations were assessed by flow cytometric analysis of CD4 and CD8 expression (n=6).

Figure 4. Single cell gene expression analysis of iPSC-Tregs.

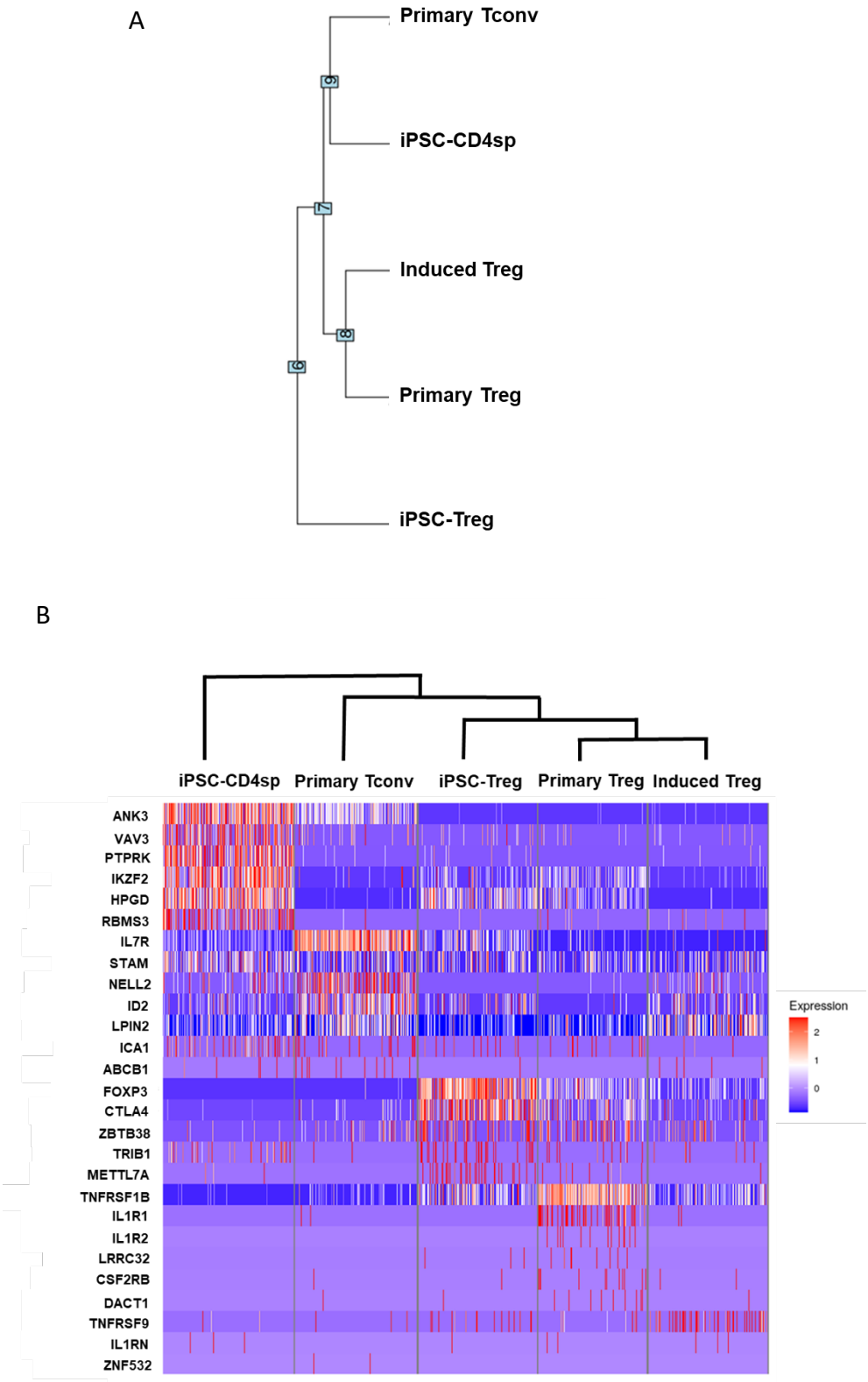

Figure 4. Single cell gene expression analysis of iPSC-Tregs.

A. Hierarchical clustering of iPSC-Tregs, iPSC-CD4sp Tcells, cultured primary T conventional (Tconv), cultured primary Treg and induced Tregs based on differentially expressed genes (DEGs). DEGs with fold change <2 and p value<0.05, were subjected to CLC analysis to perform clustering.
B. scRNA-seq heatmap showing hierarchical clustering of a core Treg gene signature in iPSC-Tregs, iPSC-CD4sp, cultured primary Tregs, induced Tregs, and cultured primary Tconv.

FIGURE 5. Characterization of sorted and activated iPSC-CD4sp and iPSC-Tregs.

A

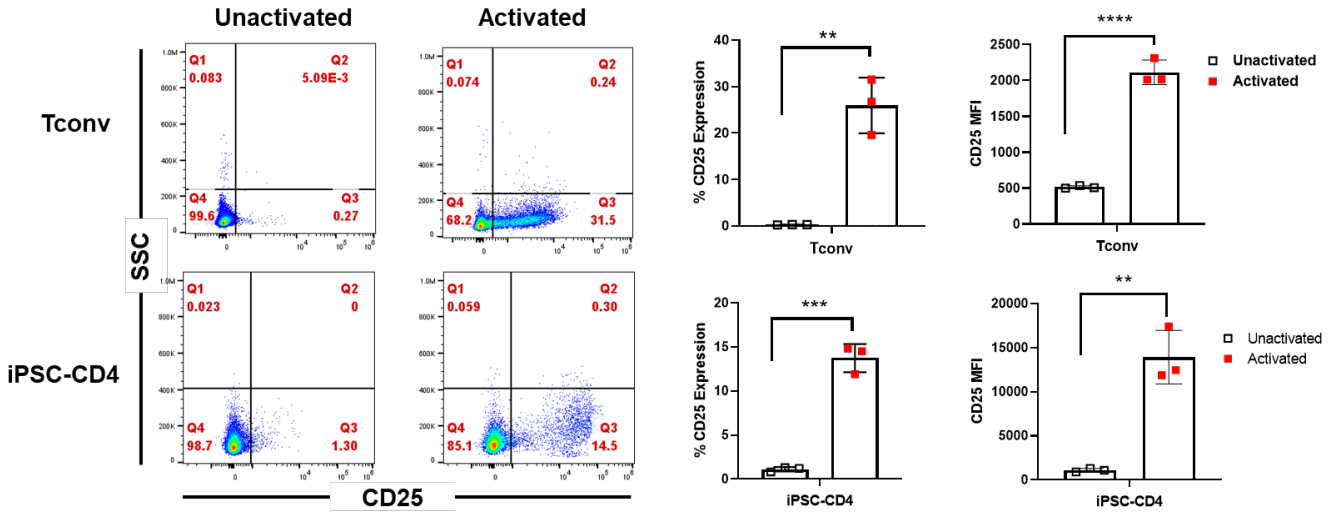

B

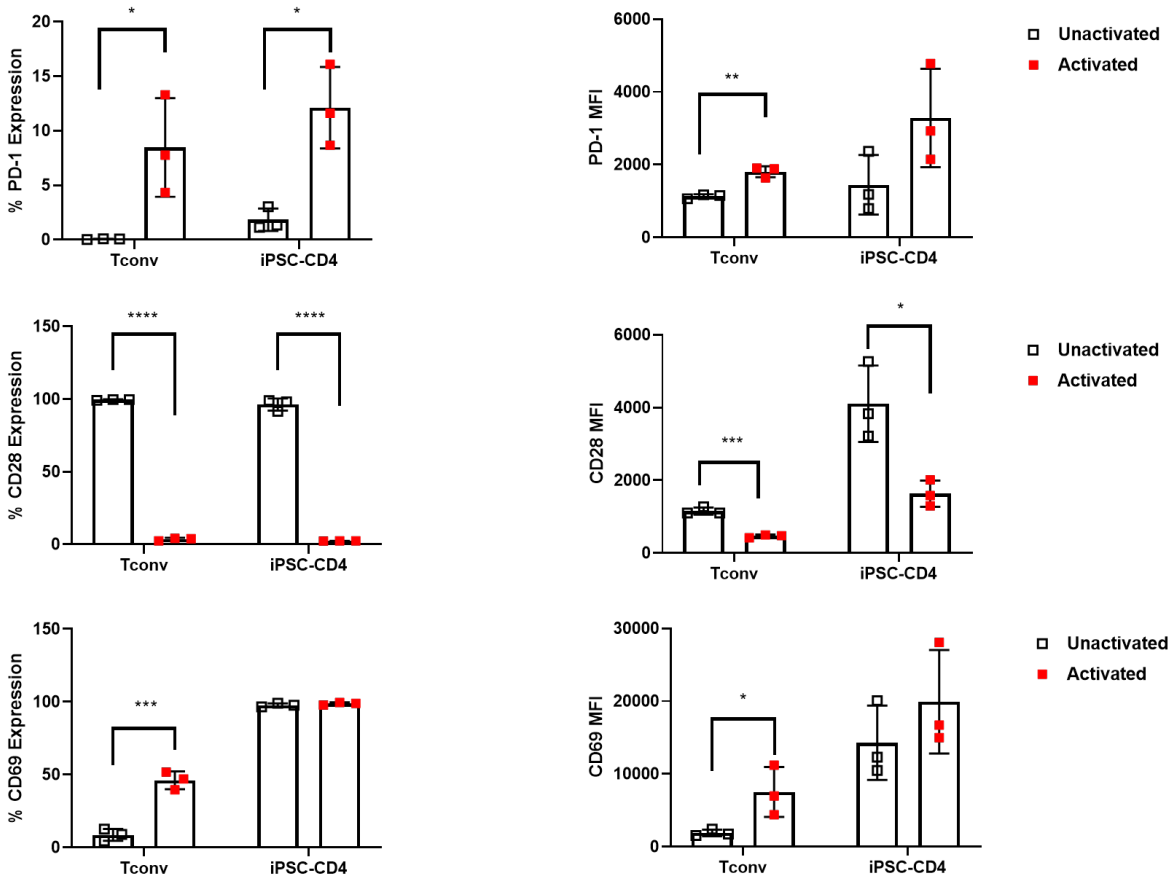

C

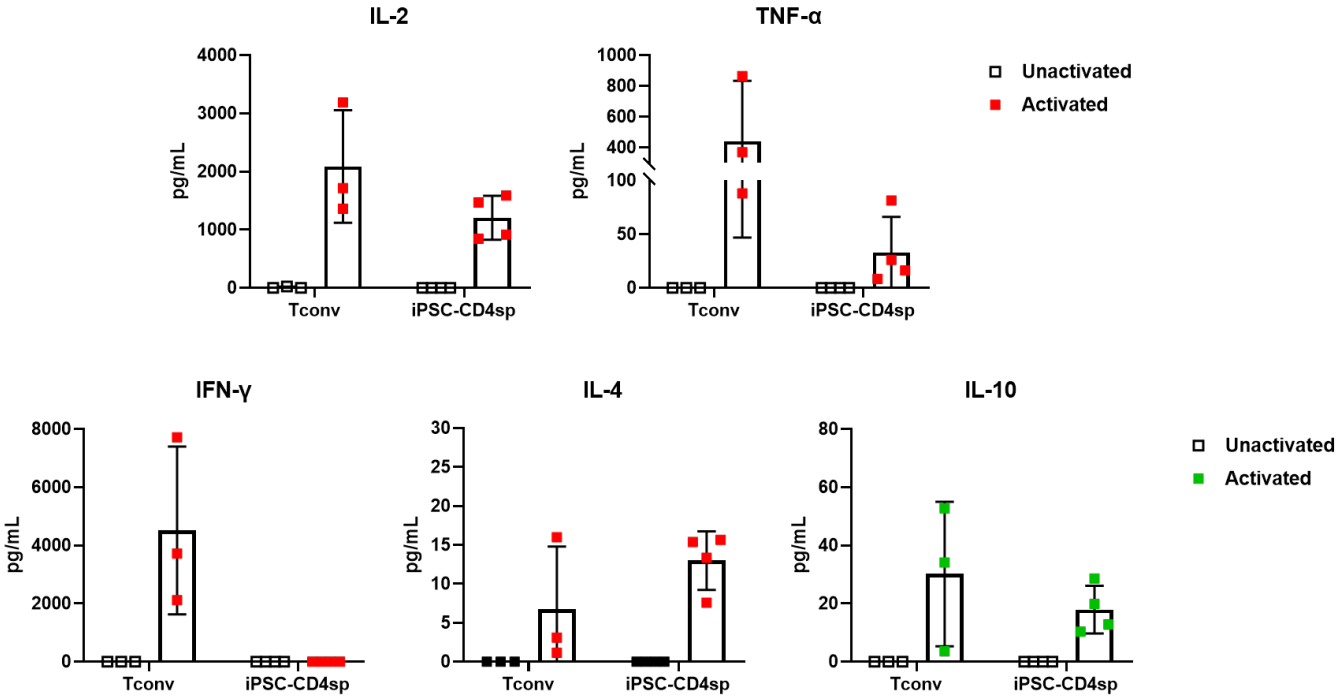
IL-2
TNF-α
IFN-γ
IL-4
IL-10
pg/mL
Tconv
iPSC-CD4sp
Unactivated
Activated

D

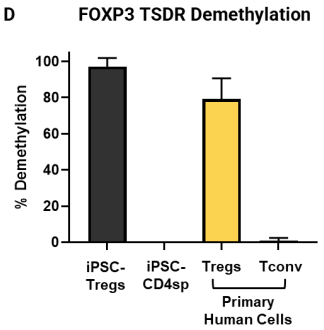
FOXP3 TSDR Demethylation
% Demethylation
iPSC-Tregs
iPSC-CD4sp
Tregs
Tconv
Primary Human Cells

E

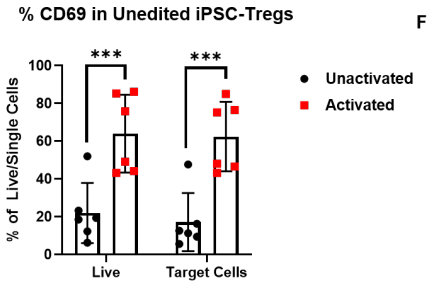
% CD69 in Unedited iPSC-Tregs
% of Live/Single Cells
***
***
Live
Target Cells
Unactivated
Activated

F

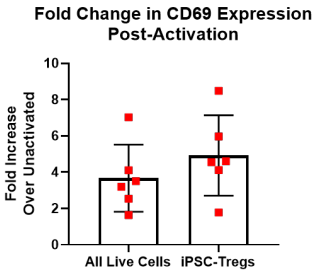
Fold Change in CD69 Expression Post-Activation
Fold Increase Over Unactivated
All Live Cells
iPSC-Tregs

G

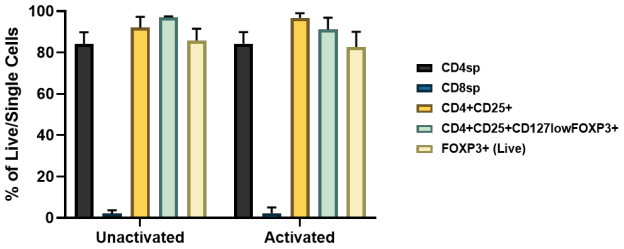
% of Live/Single Cells
Unactivated
Activated
CD4sp
CD8sp
CD4+CD25+
CD4+CD25+CD127lowFOXP3+
FOXP3+ (Live)

Figure 5. Characterization of sorted and activated iPSC-Tregs.

A. Representative flow plots and expression of CD25 in sorted unactivated and activated iPSC-CD4sp T cells or T conventional (Tconv) cells (n=3) by flow cytometry after 48 hours. CD25 Median fluorescence intensity (MFI) was calculated (right).
B. Expression of activation markers (CD69, PD-1 and CD28) was assessed by flow cytometry after 48 hours of activation. MFI was calculated (right).
C. Secretion of cytokines from sorted unactivated and activated iPSC-Tregs 24 hours after activation (n=3, iPSC-CD4sp; n=3, primary Tconv).
D. Assessment of FOXP3 TSDR demethylation in iPSC-Tregs, primary Tregs, and primary Tconv. Post-sort iPSC-Tregs were collected at day 57 for analysis and compared to primary controls (n=4, iPSC-Tregs; n=3, primary Tregs; n=3, primary Tconv).
E. Expression of Treg markers in sorted unactivated and activated iPSC-Tregs. Phenotype was assessed by flow cytometric analysis (n=6, unactivated and activated). ***$p<0.001$
F. Expression of CD69 in sorted unactivated and activated iPSC-Tregs. The expression of CD69 was assessed in both total live cell populations and target iPSC-Tregs by flow cytometry (left). Fold change in CD69 expression was assessed in activated total live and target iPSC-Tregs compared to unactivated total live cells and iPSC-Tregs (right, n=6, unactivated and activated).
G. Phenotype of unactivated and activated iPSC-Tregs. Treg markers were assessed by flow cytometric analysis (n=6).

Figure 6. Functional analysis of iPSC-Tregs.

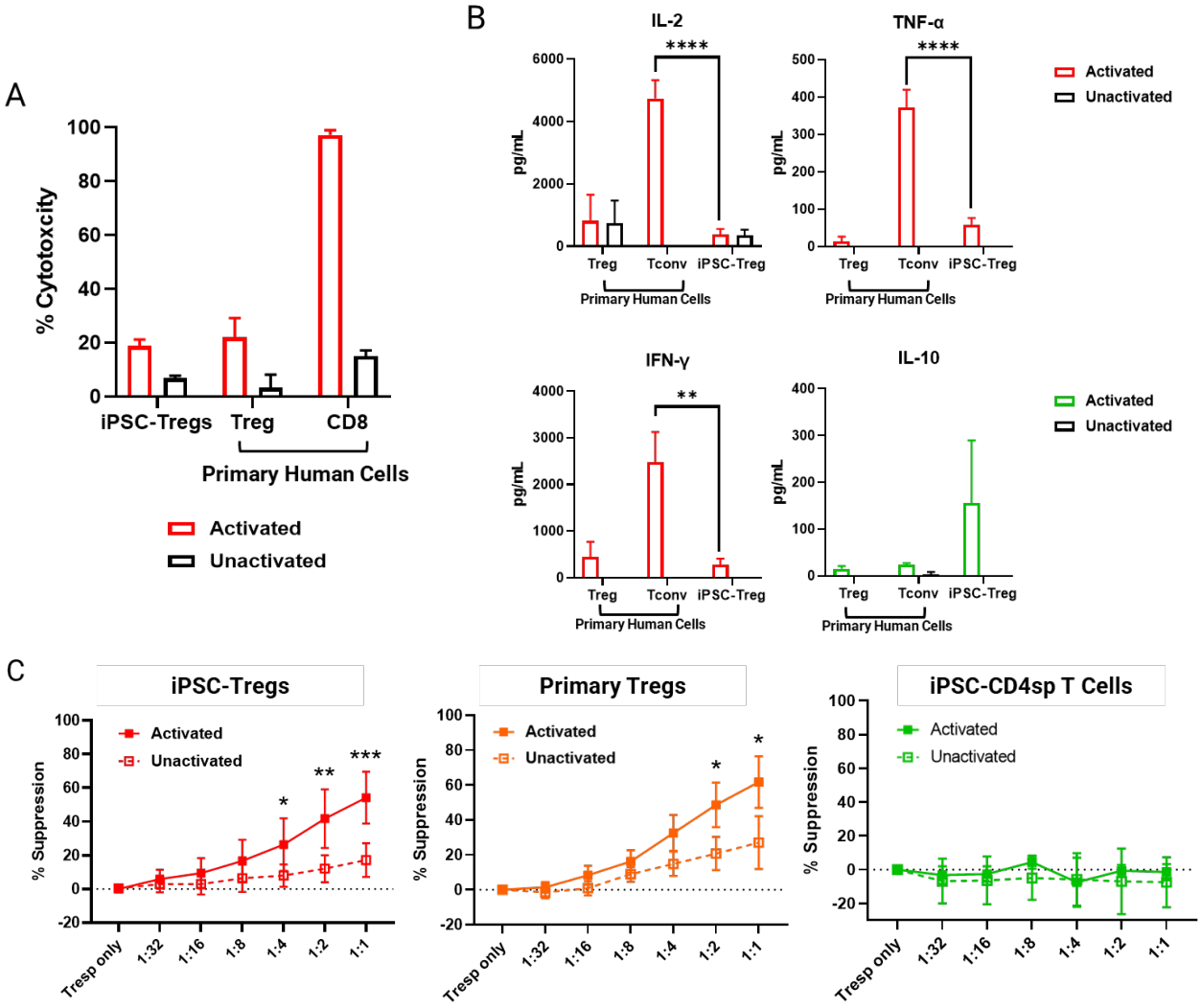

Figure 6. Functional analysis of iPSC-Tregs.

A. Cytotoxic activity of sorted unactivated and activated iPSC-Tregs as measured by an LDH release assay. iPSC-Tregs, primary Tregs, and primary CD8 T cells were cocultured with T conventional (Tconv) cells and LDH was measured after 3 days (n=3, iPSC-Tregs; n=3, primary Tregs; n=2, primary CD8 T cells).

B. Secretion of cytokines from sorted unactivated and activated iPSC-Tregs 24 hours after activation (n=4, iPSC-Tregs; n=3, primary Tregs; n=3, primary Tconv). ****p<0.0001; **p=0.0011.

C. Suppression of Tconv proliferation by unactivated and activated iPSC-Tregs, iPSC-CD4sp T cells and primary Tregs. iPSC-Tregs, primary Tregs, and iPSC-CD4sp T cells were cocultured with activated CTV labeled Tconv and CTV dilution was measured by flow cytometry after 3 days (n=6, iPSC-Tregs; n=4, primary Tregs; n=3, iPSC-CD4sp). ***p=0.0006; **p<0.001; *p<0.05.

FIGURE 7. Generation and Characterization of HLA-A2 CAR iPSC-Tregs

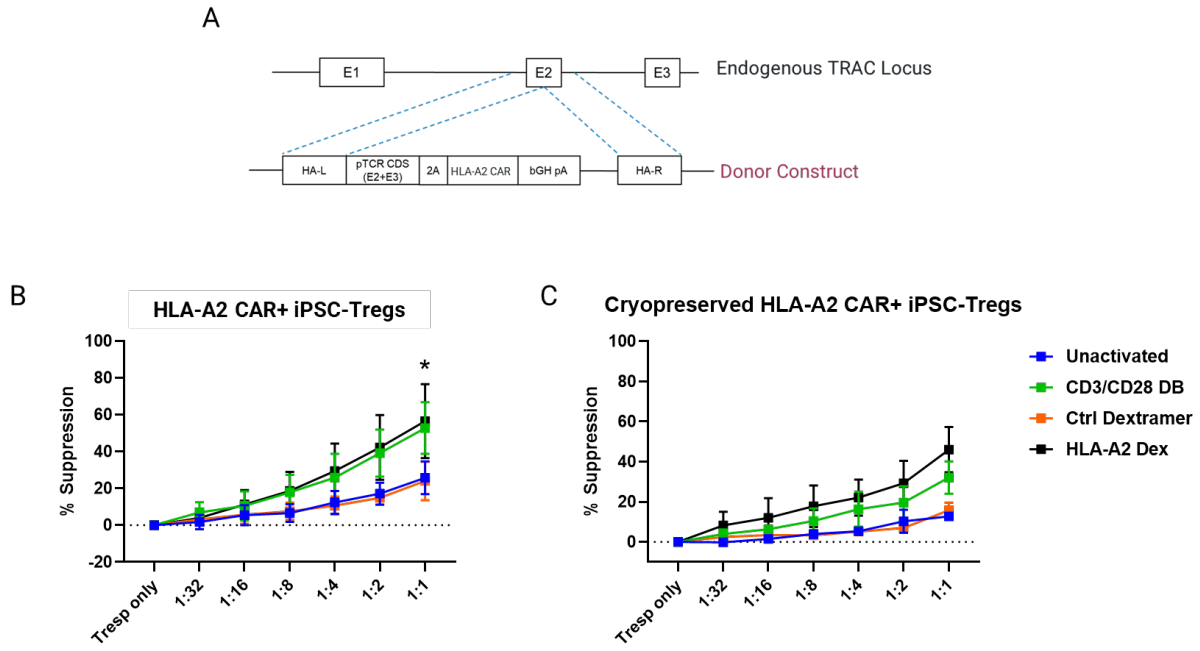

Figure 7. Generation and characterization of HLA-A2 CAR iPSC-Tregs.

A. Editing strategy for generation of HLA-A2 CAR iPSCs. A donor construct showing the TCR coding sequence and HLA-A2 CAR sequence flanked by homology arms targets exon 2 of the endogenous T Cell Receptor Alpha Constant (TRAC) locus.
B. Suppression of T conventional (Tconv) cell proliferation by HLA-A2 CAR+ iPSC-Tregs activated *via* the TCR or CAR. HLA-A2 CAR+ iPSC-Tregs were cocultured with activated CTV labeled Tconv and CTV dilution was measured by flow cytometry after 3 days (n=4). *$p<0.05$
C. Suppression of Tconv proliferation by cryopreserved HLA-A2 CAR+ iPSC-Tregs activated via the TCR or CAR. HLA-A2 CAR+ iPSC-Tregs were cocultured with activated CTV labeled Tconv and CTV dilution was measured by flow cytometry after 3 days (n=2).

SUPPLEMENTARY FIGURES

SUPPLEMENTAL FIGURE 1. Characterization of iPSCs

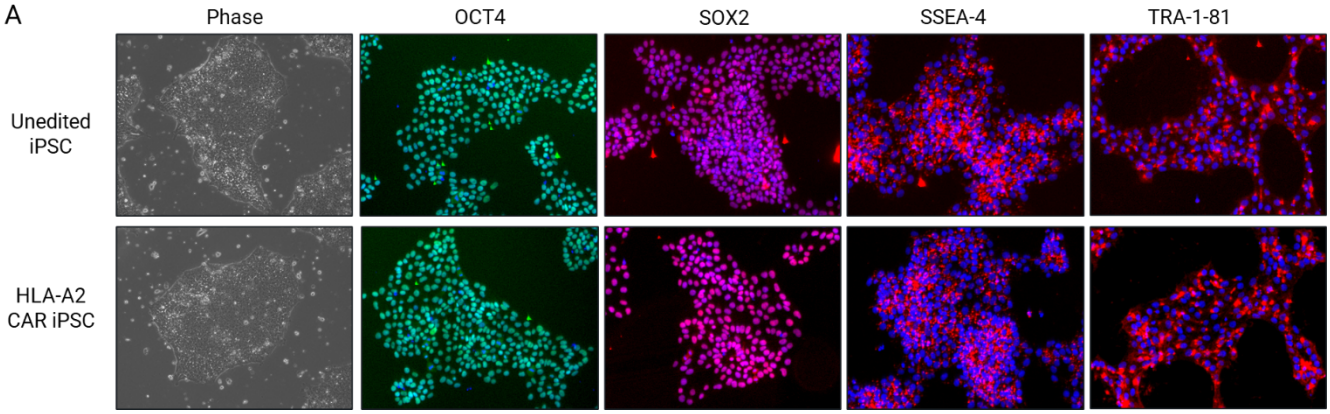

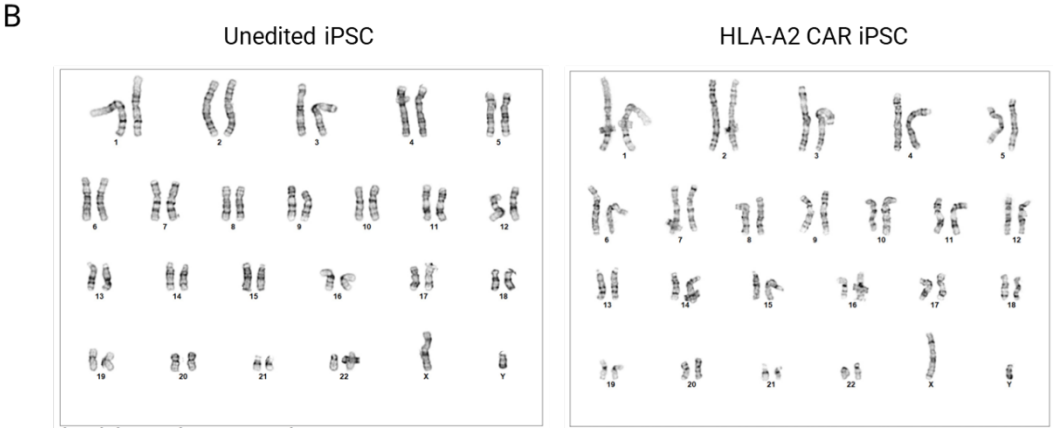

Supp. Figure 1. Characterization of iPSCs.

A. Representative images of T cell-derived iPSCs and HLA-A2 CAR edited iPSCs. iPSCs were assessed for morphology by phase contrast microscopy and expression of OCT4, SOX2, SSEA-4, and TRA-1-81 by immunocytochemistry.
B. G-band karyotyping analysis confirming normal 46 XY karyotype in T cell-derived iPSCs and HLA-A2 CAR-edited iPSCs.

SUPPLEMENTARY FIGURE 2. Double positive (DP) T Cell Yield from Unedited and HLA-A2 CAR iPSCs with CXCL12 and p38i Treatment.

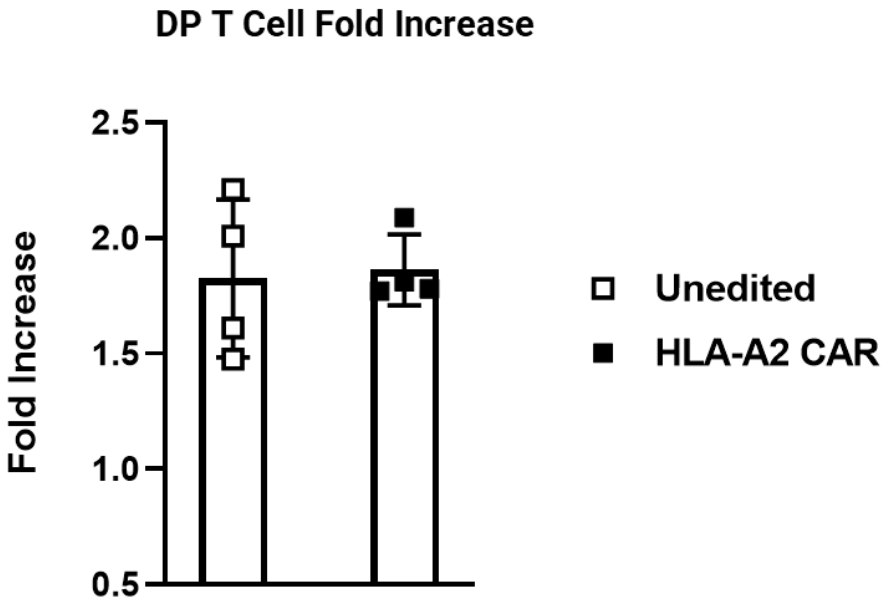

Supp. Figure 2. Double positive (DP) T cell yield from Unedited and HLA-A2 CAR iPSCs with CXCL12 and p38i treatment.
Yield of DP T cells from unedited and CAR edited iPSCs after 42 days of differentiation. CXCL12 and p38i were added at day 28 of differentiation (n=4, unedited; n=4, HLA-A2 CAR).

SUPPLEMENTAL FIGURE 3. Sorting Strategy for iPSC-CD4sp and for iPSC-Tregs

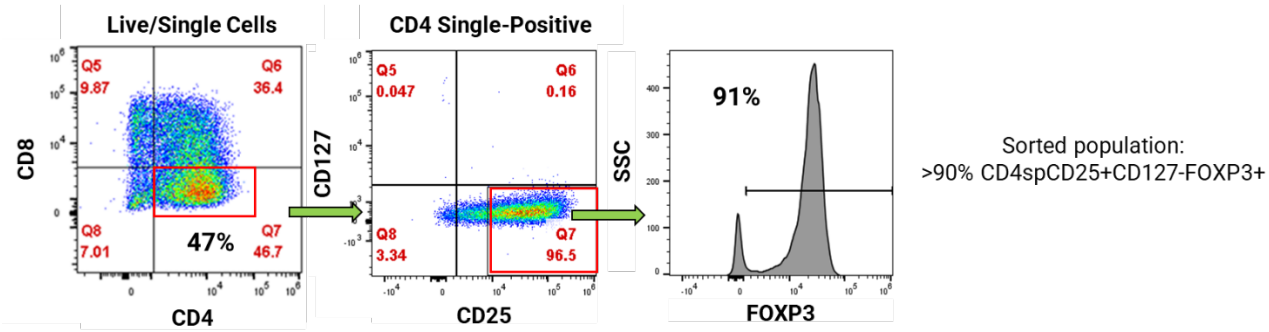

Supp. Figure 3. Sorting strategy for iPSC-CD4sp T cells and iPSC-Tregs.

Supp. Figure 4. Characterization of sorted and activated iPSC-CD4sp.

A

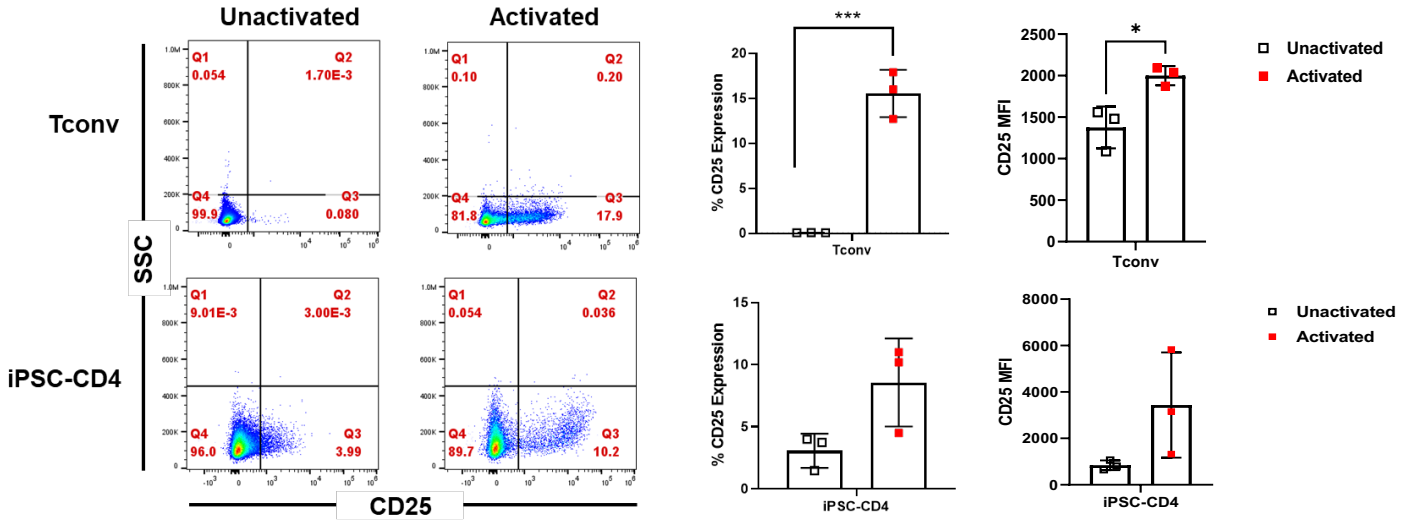

B

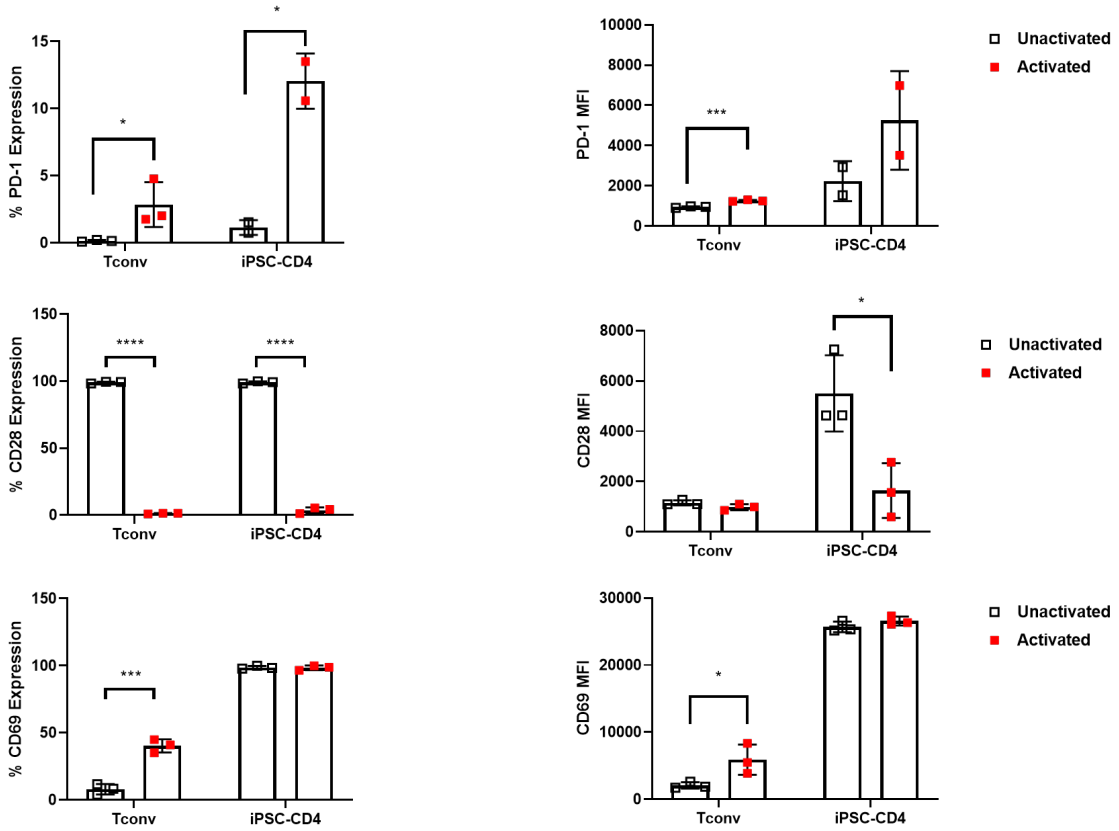

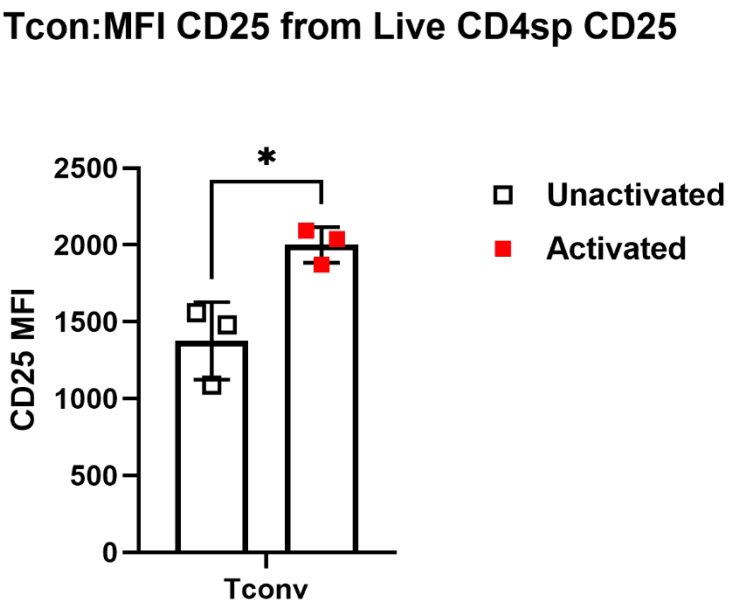

Supp. Figure 4. iPSC-CD4sp T cell characterization activation markers at 24 hours post-stimulation

A. Representative flow plots and expression of CD25 in sorted unactivated and activated iPSC-CD4sp T cells or T conventional (Tconv) cells (n=3) by flow cytometry. CD25 Median fluorescence intensity (MFI) was calculated (right).
B. Expression of activation markers (CD69, PD-1 and CD28) was assessed by flow cytometry after 24 hours of activation. MFI was calculated (right).

SUPPLEMENTARY FIGURE 5. Characterization of HLA-A2 CAR+ iPSC-Tregs pre-sort

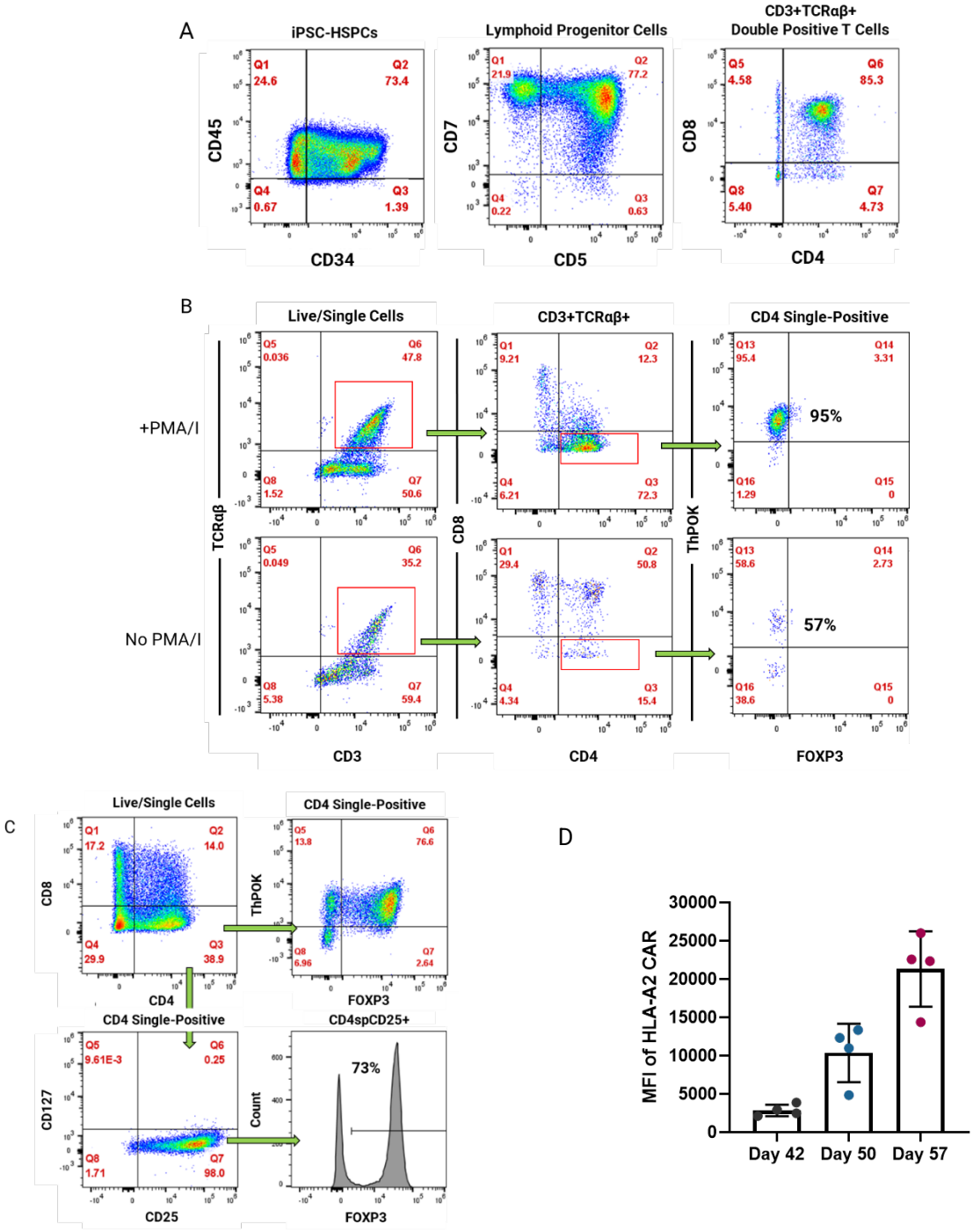

Supp. Figure 5. Characterization of HLA-A2 CAR+ iPSC-Tregs

A. Representative flow cytometric plots of hematopoietic stem and progenitor cells (HSPCs), lymphoid progenitor cells, and double positive (DP) T cells from HLA-A2 CAR edited iPSCs (n=3).
B. Representative flow plots of iPSC-CD4sp T cells 8 days after PMA/I addition (day 50 of differentiation). Phenotype was assessed by the expression levels of CD3, TCRαβ, CD4, CD8, FOXP3 and ThPOK in cells with and without PMA/I treatment (n=3).
C. Representative flow plots of iPSC-Tregs 7 days after TGFβ+ATRA addition (differentiation day 50). CD4sp phenotype was assessed by the expression levels of CD3, TCRαβ, CD4, CD8, FOXP3 and ThPOK (n=3). Treg phenotype was assessed by the expression levels of CD4, CD8, CD25, CD127, and FOXP3 (n=3).
D. MFI of CAR expression as measured at differentiation days 42, 50, and 57.

SUPPLEMENTARY FIGURE 6. Characterization of sorted HLA-A2 CAR+ iPSC-Tregs

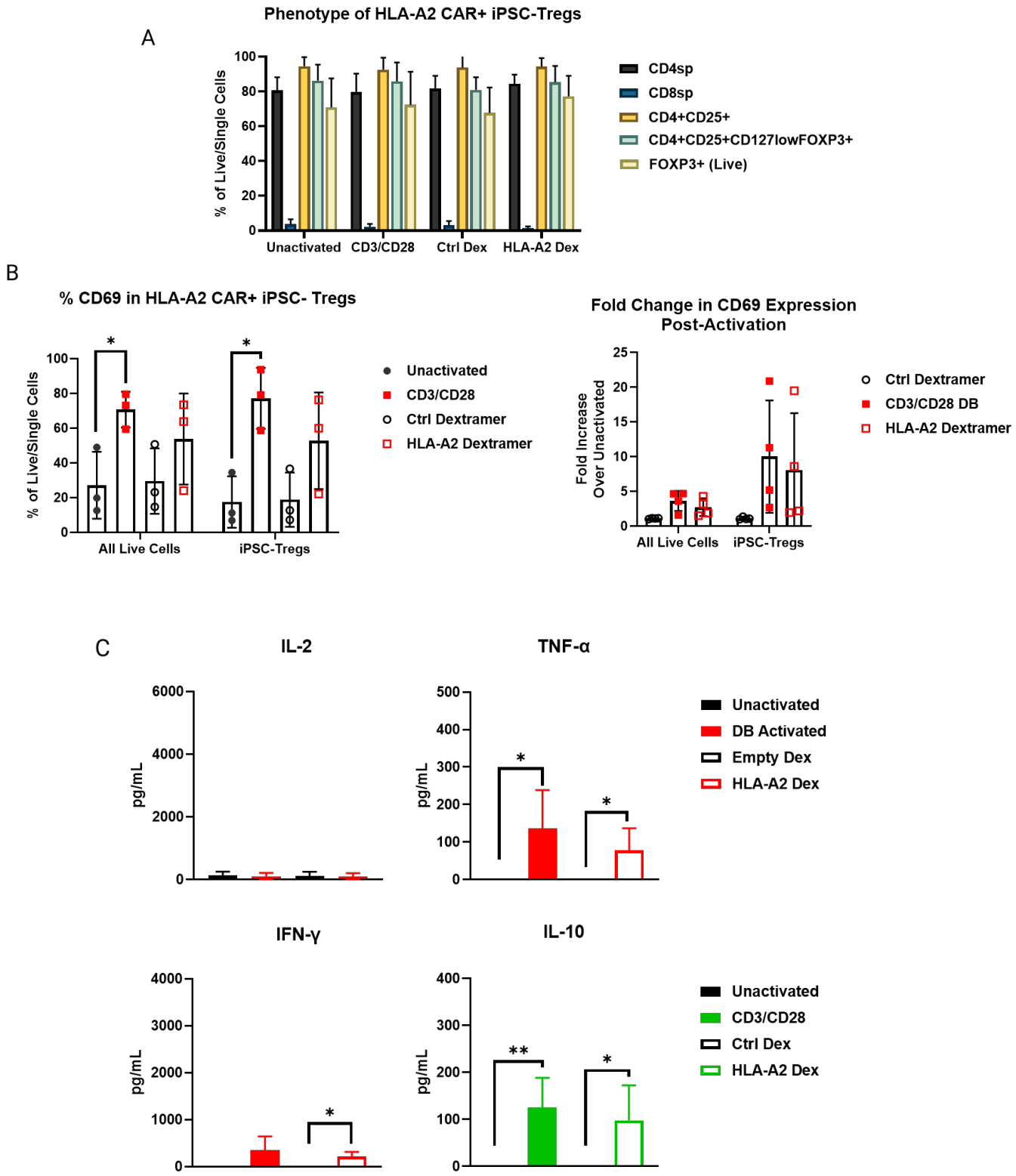

Supp. Figure 6. Functional characterization of HLA-A2 CAR+ iPSC-Tregs

A. Expression of Treg markers in sorted unactivated or control dextramer activated HLA-A2 CAR+ iPSC-Tregs and HLA-A2 CAR+ iPSC-Tregs activated via the TCR (CD3/CD28) or HLA-A2 CAR (HLA-A2 dextramer). Phenotype was assessed by flow cytometric analysis (n=4).
B. Expression of CD69 in sorted unactivated or control dextramer activated HLA-A2 CAR+ iPSC-Tregs and HLA-A2 CAR+ iPSC-Tregs activated via the TCR or HLA-A2 CAR. The expression of CD69 was assessed in both total live cell populations and target iPSC-Tregs by flow cytometry (left). Fold change in CD69 expression was assessed in activated total live and target iPSC-Tregs compared to unactivated total live cells and target iPSC-Tregs (right, n=4). *$p<0.05$.
C. Secretion of cytokines from sorted unactivated or control dextramer activated HLA-A2 CAR+ iPSC-Tregs and HLA-A2 CAR+ iPSC-Tregs activated via the TCR or HLA-A2 CAR (n=4, iPSC-Tregs).

SUPPLEMENTARY FIGURE 7. Characterization of Cryopreserved HLA-A2 CAR+ iPSC-Tregs

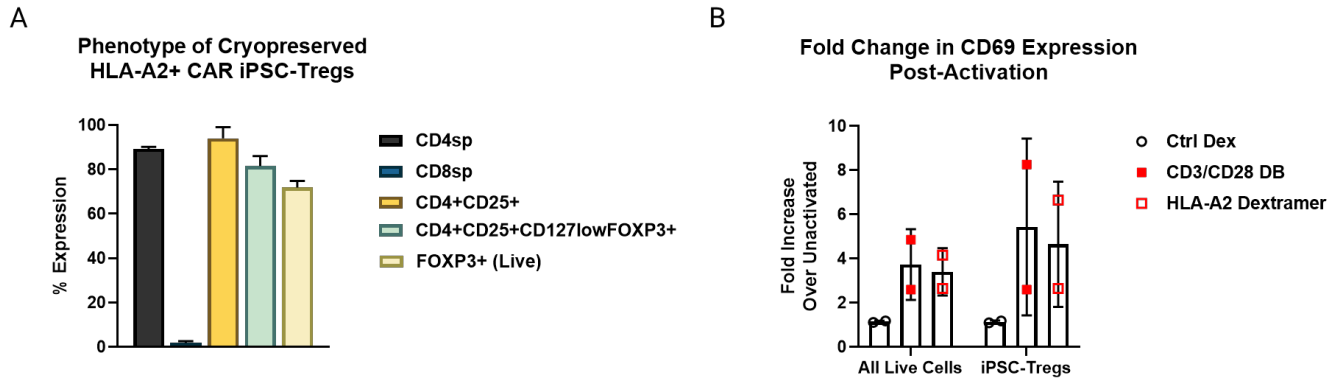

Supp. Figure 7. Characterization of Cryopreserved HLA-A2 CAR+ iPSC-Tregs

A. Expression of Treg markers in cryopreserved unactivated HLA-A2 CAR+ iPSC-Tregs. Phenotype was assessed by flow cytometric analysis (n=2).
B. Fold increase in CD69 expression was assessed in activated total live and target iPSC-Tregs compared to unactivated total live cells and iPSC-Tregs (n=2).